Group 28 Design 2 Project Report

Name	Student ID	Signature
Anthony Dongyi Yu	11527945	
Ahmed Mishqat	11550212	
Chiemezielam Samuel Ahiwe	11527747	
Gaia Liceaga Bacigalupi	11592539	
Annabel Lee	11509538	
Daria Lee	14116002	

We hereby agree that all team members have contributed equally to the work.

Submission Date: 18th December 2025

Page count: 15 pages

Word count: 6129

Task 1: Design

1.1. Z Stage Assembly

1.1.1. Right Angle Bracket

Function

The right-angle bracket is the primary structural component that supports and locates the steel workpiece on the Z-stage. It transfers all vertical loading from the workpiece into the Z-stage base and linear guides, while also providing the datum surfaces required for accurate encoder and read-head alignment. The bracket must prevent slipping, shifting, or rotation of the steel cylinder and must maintain positional accuracy under both static and dynamic loading.

Load and Service Conditions

This section summarizes the mechanical and environmental requirements that govern the design of the bracket assembly. The intent is to define the loading conditions, service environment, and interface constraints that the bracket must satisfy to ensure accurate, stable support of the steel workpiece and associated Z-stage components.

Static Load

The primary load is the weight of the steel cylinder, measured as: $F = 147\ N$. This load must be carried without yielding and without exceeding the allowable displacement of 5 μm at the top edge of the bracket.

Dynamic Loads

During rapid movements, the bracket experiences transient inertial forces. These loads are considerably smaller than the static weight but require the bracket to maintain stiffness and resist vibration to protect encoder accuracy. Dynamic effects are validated through the lead-screw torque calculations.

Service Environment

The bracket operates in a controlled laboratory environment with minimal humidity and moderate temperature variation. Materials must therefore be easy to machine, dimensionally stable and corrosion resistant or treatable. The bracket mounts directly to the Z-stage baseplate and interfaces with linear bearing housings and encoder datum surfaces. All mounting faces must be within the critical tolerances defined for the Z-stage, ensuring accurate encoder positioning and repeatable motion.

Governing Requirement: Deflection Limit

The design is governed by a simple quantitative requirement: $y_{max} \leq 5\mu m$ at the loaded top edge of the bracket. This limit ensures the workpiece position remains consistent with the Z-stage accuracy target.

Structural Model

A simplified cantilever-plate model is used for initial sizing. The vertical portion of the L-plate is treated as a cantilever of height L carrying the workpiece load at its tip. The deflection estimate is obtained using:

$$y = \frac{FL^3}{3EI} \qquad\qquad I = \frac{bt^3}{12}$$

To address the high deflection predicted by the plate model, stiffening ribs were introduced.

Effect of Stiffening Ribs

Adding two triangular ribs to the vertical plate can reduce the top-edge deflection by approximately a factor of six. This reduction factor allows thinner plates to be justified, while still meeting the 5 μm deflection requirement, thereby decreasing the weight of the Z-stage assembly and material cost.

Material Selection

Material selection for the right-angle bracket is governed by a maximum allowable elastic deflection of 5μm at the loaded top edge. Since this requirement is stiffness limited rather than strength-limited, the most appropriate preliminary screening tool is an Ashby chart of Young's modulus versus density ($E - \rho$).

Elastic deflection of a cantilever plate is inversely proportional to Young's modulus E. Therefore, materials with a high modulus will exhibit reduced deflection for a given geometry and load. However, because the bracket forms part of the moving Z-stage assembly, mass must also be minimized to limit inertial loading and motor torque requirements. This leads to the selection criterion of maximum specific stiffness, defined by the performance index: $\frac{E}{\rho}$

An $E - \rho$ Ashby chart was generated using Ansys and Mat web data for all permitted material classes. *See Figure B.4* From the Ashby chart, steels occupy the upper region of Young's modulus but at a high density, leading to increased mass and reduced suitability for a moving stage. Aluminum alloys provide a lower modulus to steel, but benefit from significantly reduced density, offering favourable stiffness-to-weight compromise. Therefore, aluminium alloys are the most appropriate candidates for meeting the deflection requirement. *See Figure B.5*

Decision Matrix

Based on this screening, aluminium and steel alloys were shortlisted for detailed evaluation using quantitative deflection calculations and a decision matrix incorporating cost, machinability and availability to select the most suitable material for the right-angle bracket. While the Ashby chart identifies materials with favourable stiffness to density ratios, it does not account for practical manufacturing and cost considerations. The decision matrix therefore provided a structured method to compare shortlisted materials using design-relevant criteria. *See Appendix B.3*

The candidate materials considered in the matrix were aluminium alloys: 20224-T3, 5052-H32, 6061-T6, 6082-T6, 7075-T6, 7475-T61 and steel: 4130 chromoly. Each material was evaluated against four key criteria:

- Elastic stiffness to strength – to ensure the 5μ deflection requirement can be met with realistic geometry
- Density – to minimise moving mass and hence reduce Z-stage motor loading
- Machinability – Including ease of CNC milling, surface finish quality and tool wear
- Cost and availability – Reflecting procurement time and suitability for student manufacturing

High-strength aluminium alloys such as 7075-T6 and 7475-T61 scored strongly in stiffness and strength, but penalised for high cost, limited availability and poorer machinability. 4160 Steel achieved high stiffness scores but was heavily penalized due to its high density which increase inertial loading and motor torque requirements on the Z-stage.

Among the materials evaluated, although 6063-T6 Al does not possess the highest strength, its elastic modulus is sufficient to meet machinability, low cost and wide availability. As a result, 6063-T6 Al was selected as the final material for the right-angle bracket.

Design

Chosen Embodiment

The right-angle bracket geometry was developed to satisfy the governing deflection requirement of 5 μm under the applied workpiece load while minimizing mass. The design load corresponds to the weight of the steel cylinder: $F = 147\ N$.

The vertical plate was conservatively modelled as a cantilever beam of height L, fixed at the base and loaded at the free end. Deflection was estimated using the model above. Thereby overestimating deflection by neglecting load sharing through the plate and ribs, providing a basis for preliminary sizing.

- **Material:** 6063-T6 Aluminium
- **Key Section Thickness:** 25 mm horizontal plate and 10 mm vertical plate
- **Stiffening Feature:** Two full-height triangular aluminium ribs joining the vertical and base plates
- **Major drive/guide:** Direct mounting to Z-stage linear bearing carriages with encoder datum surfaces machined into the vertical face

Initial calculation showed that a plate not supported would require a substantially greater thickness to meet the 5 μm limit, resulting in excessive mass. As a result, two triangular stiffening ribs were added to improve the stiffness

The rib length was selected to span the full diameter of the steel cylinder. A platform length of 320 mm was chosen, exceeding the 300 mm cylinder diameter to accommodate manufacturing tolerances, simplify assembly and allow space for optional safety features.

Using the ribbed configuration, several plate thicknesses were evaluated. A thickness of 25 mm resulted in a calculated deflection of approximately 2 μm, which is less than half the allowable limit. This provides a safety margin for vibration, manufacturing tolerance and minor dynamic effects while maintaining reasonable mass.

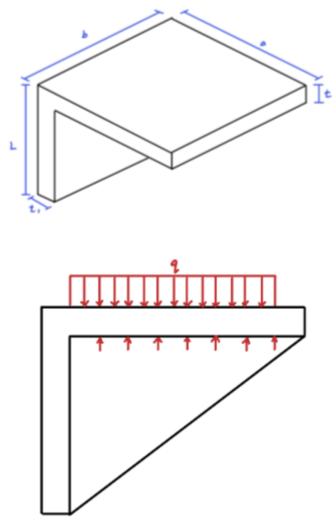

Figure 1- Dimensions and FBD of right-angle bracket for 2D analysis

Dimensions

- $L = 300mm$
- $a = 320mm$
- $b = 320mm$
- $t = 25mm$
- $t_1 = 10mm$

Free Body Diagram

- $q = 2101\ N/m$
- $y_{max} = -2.87\ \mu m$

Manufacturing

The bracket will be manufactured from a 6063-T6 aluminium plate. Raw stock is first cut oversize to form the L-shaped blank. The part is then CNC-machined to establish the primary datum faces, with the top surface as the primary datum as its directly related to the workpiece position and encoder alignment.

Mounting holes and interface features are subsequently drilled, tapped, deburred and chamfered in reference to this datum to ensure consistent alignment. The triangular ribs will be CNC-machined separately from aluminum stock to achieve accurate profiles and flat mating surfaces.

The ribs are positioned against the vertical and horizontal plates using the machined datum faces and are permanently joined using welding. If required, post-weld machining can be performed to restore flatness at the critical interfaces.

Final inspection will be conducted on a surface plate using a height gage to verify flatness and length dimensions of the primary datum surface. Dimensional tolerances of ±5 mm for plate dimensions and ±0.3 mm for rib features were selected from ISO general tolerance tables. *See Appendix B – Table 3.*

Design Evolution

The initial bracket design used a width of 250 mm, meeting the minimum functional requirement while minimizing material usage. However, design review revealed that this configuration appeared visually unstable and offered limited tolerance for assembly variation.

The width was increased to 300 mm to match the steel cylinder diameter, improved the perceived stability and load distribution. A further increase to 320 mm was implemented to allow for manufacturing tolerances, assembly ease and the inclusion of optional safety contingencies.

Although the increased width slightly increased mass and bending demand, this effect was mitigated by the introduction of triangular stiffening ribs. The final ribbed design achieved lower deflection than earlier versions while improving robustness, user confidence and manufacturability.

1.1.2. Z Stage

Function

The Z-stage provides vertical positioning of the steel workpiece and right-angle bracket relative to the Y-stage. It supports the full mass of the workpiece and bracket while maintaining high stiffness and positional accuracy during vertical motion. The bracket is bolted to the Z-axis moving plate, which is guided by two linear rails; vertical motion is generated by a leadscrew that drives an anti-backlash nut mounted to the moving plate.

Service Conditions

Vertical Travel

The Z-stage must provide 150 mm of vertical travel. This distance must be completed within 3s with each acceleration and deceleration phase not exceeding 0.5s.

Vertical Load Capacity

The Z-stage must support the combined weight of the bracket and workpiece: 245.67N static vertical load and a peak inertial load of 248.7N during upward acceleration. Applying a safety factor of 4, the minimum required load-carrying capacity of the guide and drive system must exceed 1000N.

Stiffness Target

The Z-stage components, including the plate and right-angle bracket are limited to a maximum elastic deflection in the vertical direction no greater than 5μm under the maximum design load.

Positional Accuracy and Repeatability

The Z-stage will provide high positional repeatability to ensure the steel workpiece can be consistently positioned at the laser focal plane. Any elastic deformation, backlash or vibration cannot compromise positioning accuracy during operation.

Operating Environment

The Z-stage operates in a controlled laboratory environment with low humidity and moderate temperature variation. Materials must therefore be dimensionally stable, corrosion resistant or treatable and suitable for continuous operation.

Chosen Embodiment

- **Linear Guides:** NSK PU09TR recirculating linear rails with 4 carriages
- **Lead Screw:** Trapezoidal lead screw; SRA 2-12x2M (Ø12 mm, 4 mm lead)
- **Nut:** XCF5000 flanged anti-backlash nut
- **Support Bearings:** 609 deep-groove ball bearings
- **Drive:** Maxon DCX 26L DC motor with GPX 26 planetary gearbox (5.3:2)
- **Position Feedback:** Linear optical encoder

Linear Guide Rail Selection

Load Capacity

Loads on the linear rails are generated from the combined mass of the workpiece, right-angle bracket and moving Z-stage components. Force and moment equilibrium were used to resolve the applied loads into forces acting on individual carriages under worst-case loading conditions. The load-optimal motion scenario was used to determine the maximum acceleration and corresponding inertial load, which governs the sizing of the linear rails, lead screw, bearings, motor torque, and structural stiffness of the Z-stage. *See Appendix C.1 – Figure C.1.*

The maximum horizontal force acting on the linear bearings was calculated as $F = 131.02N$. Applying a safety factor of 4 gives a design load of 524.08 N, which is shared between two carriages, resulting in 262.04N per carriage. Therefore, the selected carriage must maintain that $C > 262.04N$. The selected PU09TR carriage is the smallest and lightest PU-series option that provides a dynamic load rating of 1490 N.

Length Compatibility
The PU09TR rail was available in lengths up to 600 mm, thus exceeding the required length of 450 mm, allowing full travel with end clearances for bearing blocks and limit stops.

Lead Screw and Nut Selection

Axial Load and Torque
SRA 2-12x2M lead screw was selected
The worst-case axial load occurs during upward acceleration and was calculated as $F_a = 248.7N$. Applying the safety factor of 4 gives a conservative design load of 992 N. The required driving torque was calculated using:

$$T = \frac{F \times Lead}{2\pi\eta} = 0.29Nm$$

Buckling and Shaft Whip
Using the Thompson buckling chart, a lead screw with a minor diameter greater than 9 mm is required to prevent buckling over the 510mm unsupported length. The selected lead screw satisfies this requirement with a minor diameter of 9.2 mm. By considering the maximum linear speed would be 0.06m/s and 4 mm lead, the revolutions per minute is determined:

$$n = \frac{v}{Lead} = 900RPM$$

The shaft whip chart indicates a maximum permissible speed of 1200 rpm. The required operating speed 900<1200, Therefore, the screw selected will not buckle or whip.

Nut Selection
An XCF5000 flanged anti-backlash nut was selected for its compatibility with the lead screw diameter and lead. Additionally, it can eliminate axial play in the lead screw, ensuring high positioning repeatability.

Bearing Selection

Load Calculation and Dimensions
Deep-groove bearings were selected rather than angular-contact bearings because the lead screw experiences a large angular velocity.

Two 609 deep-groove ball bearings were selected to support the lead screw with a dynamic rating, $C_R = 3350N$ and a static rating, $C_0 = 1430N$. The safety requirement is satisfied during upwards acceleration where the maximum axial load, $F_{axial} = 248.7N$, is sufficiently below the static rating for the 609 deep-groove ball bearing.

The bearing bore diameter and minimum preferred shoulder diameter is restricted to less than 9.2 mm, the leadscrew minor diameter, so that the leadscrew can be machined down to fit the bearings. Ideally, 9 mm bore diameter is optimal to minimise waste during machining, while retaining the leadscrew load ratings. After considering all bearings with inner diameter of 9 mm, only 609 and 629 meet the radial load requirements. 609 was chosen because it is lighter and has a smaller shoulder diameter than 629. *See Appendix C.4 – Bearing Selection*.

Life Calculations
The bearing fatigue life was evaluating using the basic rating life L_{10}, which represents the number of operating hours at which 90% of identical bearings are expected to operate without failure under ideal conditions. The selected 609 deep groove bearing yields a bearing life of approximately 3,520 hrs which is beyond sufficient for the application of this project, meaning the fatigue life is not a limiting factor for the Z-stage design, confirming suitability for continuous operation. *See Appendix C – Bearing Selection*

Motor and Gearbox Selection

The minimum mechanical power requirement for the lead screw is $P = 27.3\ W$, calculated using: $P = T\omega$

As a result, the Maxon DCX 26L with graphite brushes, ball bearings motor was selected rated to generate 40W of power. From the Maxon catalogue, this motor is rated to offer a no-load speed of $\omega_0 = 10700\ rpm$ and a nominal torque of $T_N = 57.8\ mNm$ with a stall torque of $T_S = 695\ mNm$. Additionally selected was the GPX 26 mm, 1-stage planetary gearbox with a 5.3:1 reduction ratio. The combined efficiency is approximately 81% with a €385.25 total cost being lower cost and lower power requirements than just buying a singular more powerful motor like the DCX 32L.

Operating Point Verification

The operating point of the motor-gearbox combination was plotted on the torque-speed diagram (*Appendix C.6*). The required operating point lies within the continuous operation region and corresponds to a reduced thermal resistance. This ensures that Z-stage operation will be reliable without overheating.

Plate and Stage Deflection

The Z-stage is modelled as a cantilever fixed at the Y-stage interface. Forces transmitted through the right-angle bracket generate a horizontal couple acting on the stage through the bearing carriages.

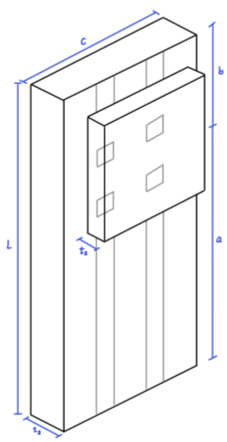

Figure 2- Dimensions of Z-stage

Dimensions

- $t_2 = 0.001m$
- t_3 =0.054m
- c =0.36m
- a =0.17m
- $b = 0.36m$
- $L = 0.53m$

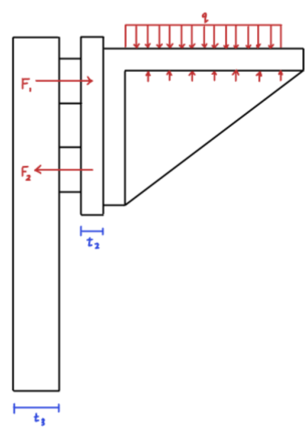

Figure 3- FBD of Z-stage for reaction force analysis

Free Body Diagram

- $F_1 = 131.02\ N$
  $F_2 = -131.02\ N$

From the force analysis of the Z-stage assembly, the horizontal force acting on the linear bearings is $F = \pm 131.02N$, applied as a couple across four carriages separated by a vertical distance of 300 mm. This produces a bending moment, resulting in elastic deflection at the top edge.

Deflection Results and Stiffness Compliance

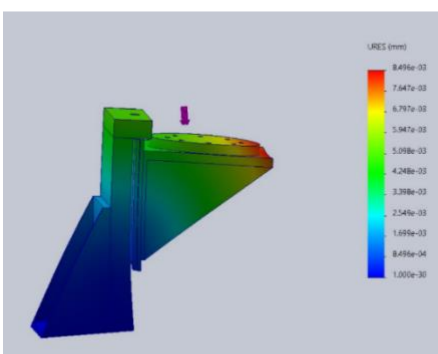

Figure 4- SolidWorks simulation of Z-stage deflection

Without stiffening ribs, the calculated deflection remained below 30 μm, meeting the preliminary stiffness requirement. With the inclusion of two triangular ribs, the maximum deflection was reduced to 3.745 μm, satisfying the final stiffness requirement $y_{max} \leq 5\mu m$. This confirms that the rib-enforced embodiment is required to meet the Z-stage stiffness target. *See Appendix C – Stage Deflection*.

Manufacturing

The plate, stage and ribs are machined from Aluminium 6063-T6. Datum faces are established during CNC machining to control Z-axis straightness and alignment. Ribs will be welded to the stage, with post-weld machining used to restore flatness where required.

Design Evolution

Early iterations used smaller stage width and thickness, resulting in deflections close to the allowable limit. Increasing stage width to 330 mm and thickness to 54.2 mm increased bending stiffness and reduced deflection to 3.745 µm. The addition of ribs further improved stiffness without significant increases in mass or manufacturing complexity.

Final Design Description

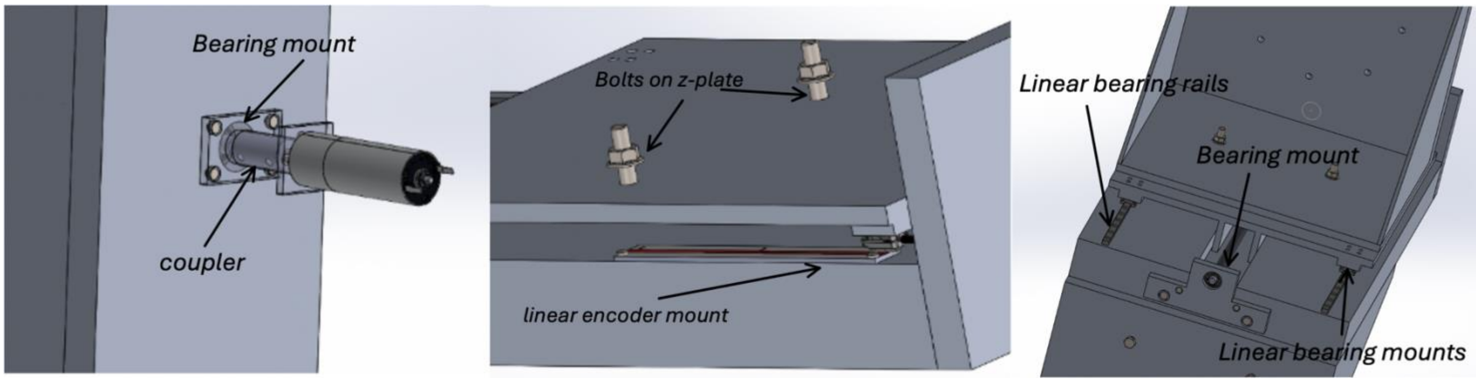

Figure 5- Details of Z stage mounting arrangements

1.2. The Y Stage

Function

The Y-stage provides horizontal translation of the Z-stage assembly, including the vertical plate, right angle bracket, workpiece and associated drive components. The Z-stage is mounted directly onto the Y-stage and all loads generated by the Z-stage are transmitted into the Y-stage structure and linear guide system. Thus, the Y-stage must support a combination of vertical loads and bending moments while maintaining adequate stiffness, smooth motion and positional accuracy.

Service Conditions

Applied Loads

The Y-stage supports the entire Z-stage assembly and workpiece. Therefore, it experiences significant vertical loading transmitted through the linear guide system. Loads are generated by the vertical stage weight and reaction forces from the overturning moments. These loads are distributed across two parallel linear rails and their associated recirculating carriages. Static equilibrium analysis converts these moment loads into equivalent rail forces.

Based on load distribution analysis, the worst-case force acting on the system, the combined effect of the moment-induced forces and vertical weight result in a maximum load of 773.86 N per rail. Therefore, the maximum load per carriage is $F = \pm 386.93\ N$. To ensure reliable operation and to account for uncertainties in loading, alignment and manufacturing tolerances, a safety factor of 4 was applied. As a result, the required carriage load capacity is $F_{design} = 1589.72\ N$. *See Appendix D – Load Determination*.

Horizontal Travel Range

The minimum required Y-axis travel is 350 mm. In addition, the Z-stage base length is 255 mm and must be mounted on the Y-stage, resulting in a minimum required rail length of 605 mm. The selected linear guide must therefore be available in a length greater than this value.

Chosen Embodiment

- **Linear Guides:** NSK PU12TR recirculating linear rails with 4 carriages
- **Lead Screw:** Trapezoidal lead screw; SRA 7-16x2.3M (Ø16 mm, 16 mm lead)
- **Nut:** XCF6200 flanged anti-backlash nut
- **Support Bearings:** NSK 6300 deep-groove ball bearings
- **Drive:** Maxon DCX 19 DC motor (24V) with GPX 14 mm planetary gearbox (6.6:1)
- **Position Feedback:** Linear optical encoder

Linear Guide Rail Selection

Load Capacity

The PU12TR linear rail system was selected for the Y-stage. This rail offers statistic and dynamic load ratings that comfortable exceed the required design load, $F_{design} = 1547.72\ N$ per carriage.

The alternative rail options, such as the PU12UR, were considered. However, these alternatives were heavier and more expensive without providing meaningful performance benefits over the PU12TR for this application. Ultimately, the PU12TR rail was selected because it represents the most efficient balance of load capacity, size, weight and cost. *See Appendix D.2 Load Calculation of Linear Rails.*

Length Compatibility

Furthermore, the PU12TR rail is available in lengths up to 800 mm, which sufficiently satisfies the geometric travel requirement of 605 mm.

Lead Screw and Nut Selection

Axial Load and Torque

SRA 7-16x2.3M leadscrew was selected.
The Y-stage motion profile was defined by the requirement to complete a 350 mm horizontal travel within 3 seconds. From the specified acceleration and deceleration limits, the maximum linear speed and acceleration were determined. Since the Y-stage motion does not act against gravity, the required axial force is significantly lower than that of the Z-stage. (*See Appendix D.1*).

The force required to drive the Y-stage was determined using Newton's second law:

$$F = ma$$

The resulting driving force was found to be $F = 19N$. A safety factor of 4 was applied to the design load for design checks related to buckling and shaft stability, therefore, $C_a > 76\ N$.
The corresponding driving torque for a lead screw is given by:

$$T = \frac{F \times Lead}{2\pi\eta}$$

Resulting in a required torque of $T = 0.0645\ Nm$.
Since the Y-stage must travel a greater distance than the Z-stage within the same time constraint, a lead screw with a larger lead was selected to reduce the required rotational speed while maintaining reasonable torque demands.

Buckling and Shaft Whip

The torque required to drive the lead screw was calculated using the standard screw torque relationship applied in the Z-stage, accounting for the applied axial force, lead screw and efficiency. The corresponding rotational relationship was determined from the required linear velocity and lead screw. These calculations confirm that the operating speed of the lead screw was calculated to be $n = 525\ rpm$ (*See Appendix D – Force and Motion Calculations*).

At this rotational speed, shaft whip was assessed using standard critical speed charts for the selected bearing arrangement. The analysis shows that a lead screw of 8 mm or greater would be sufficient to ensure that the operating speed remains below the critical shaft whip speed for the given screw length. (*See Appendix D – Figure D.3*).

Buckling was evaluated under compressive loading using a compressive safety factor of 4. The analysis indicates that a minimum diameter of 10 mm is required to prevent buckling and therefore the selected 16 mm diameter lead screw is within the acceptable limits. This diameter provides sufficient buckling resistance while remaining compatible with the limited torque output of a high-speed DC motor. Larger lead values were ignored due to excessive torque demand, making the selected leadscrew an optimal choice. (*See Appendix D – Figure D.4 & Table D.2*).

Nut selection

The XCF6200 flanged nut was selected for this case. This nut is fully compatible with 16 mm screw diameter and lead, provides convenient mounting features for attachment to the Y-stage plate and incorporates preload to reduce backlash. The use of a preloaded nut improves positioning accuracy and repeatability, which is essential for maintaining alignment between the Y-stage and the overlying Z-stage.

Bearing Selection

Load Determination and Dimensions

Under load-optimal case scenario assumptions, the axial load calculated to be $F_{Axial} = 19.0\ N$, while the radial load which is the weight of the Z-stage assembly is $F_{Radial} = 665.5\ N$. Since the load ratio $F_a/F_r = 0.029 < 0.5$, the equivalent dynamic load is governed by the radial load alone. Applying a safety factor of 4 gives an equivalent design load of $F_{eq} = 2662\ N$.

Deep-groove ball bearings were selected as they are well-suited for high rotational speed and large radial loads. The NSK 6300 series deep-grooved ball bearing was selected because its static and dynamic load ratings exceeded the required design load (*See Appendix D – Table D.3*). Additionally, its 10 mm bore diameter is compatible with the machine lead screw diameter (*See appendix D – Table D.*4). Furthermore, the bearing offers a compact form when compared to the 6800 series, while 6200 series did not offer a suitable minimum diameter below 12 mm.

Life Calculation

Bearing life calculations indicate an expected life of 4423 hrs, which is significantly greater than the required operational life of the system. Therefore, the fatigue life is not a limiting factor for the Y-stage design, confirming suitability for continuous operation. *See Appendix D.4 – Bearing Selection*

Motor and Gearbox Selection

The torque and speed requirements of the Y-stage lead screw do not need to be directly met by the motor if a gearbox is employed. A motor-gearbox configuration is therefore used because the system has excess available angular speed and relatively low torque demand. This approach allows the use of a smaller rotor, reducing overall size, electrical power consumption and thermal loading while maintaining adequate performance.

Maxon DCX 19 DC motor (24 V) was selected for the Y-stage drive. This motor provides a no-load speed of $\omega_0 = 12700\ rpm$, a nominal torque of $T_N = 11.4\ mNm$, and a stall torque of $T_S = 74.6\ mNm$. The motor is coupled to a GPX 14 mm single-stage planetary gearbox with a reduction ratio of 6.6:1. The combined motor gearbox efficiency is approximately 81% and a €261.36 total assembly cost.

Operating Point Verification

The required operating conditions at the lead screw are a torque of $T = 64.5\ mNm$ and a rotational speed of $\omega = 525\ rpm$. With the selected gearbox, the output torque is increased and the angular speed reduced by the reduction ratio. Accounting for gearbox efficiency, the corresponding motor operating point is approximately $10.9\ mNm$ at 3465 rpm. This operating point lies within the nominal region of the motor speed-torque diagram and within the continuous operation envelope, confirming that the motor can operate reliability without risk of overheating. *See Appendix D – Table D.5, Figure D.5 and Figure D.6.* Alternative motors were rejected due to voltage incompatibility issues. *See Appendix D – Figure D.4*.

Plate and Stage Deflection

The stiffness of the Y-stage plate was evaluated by considering deflection due to both the self-weight of the plate and the applied forces transmitted from the Z-stage. The plate was modelled using beam theory and superposition was applied to account for combined effects of a uniformly distributed load and two concentrated forces F_3 and F_4. *See Appendix D for full worked solutions.*

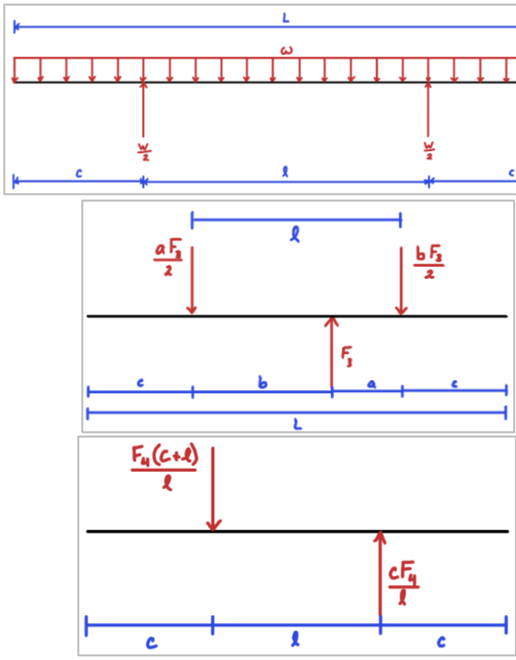

Figure 6,7,8- FBD and dimensions of Y axis

Free Body Diagram for Uniform Load

- $y_{uniform} = \frac{W(l+c)}{24EIL}\left[3c^2(c+2l) - l^3\right]$

Free Body Diagram for F_3

- $y_{F_3} = \frac{F_3 abc}{6El}(l+b)$

Free Body Diagram for F_4

- $y_{F_4} = \frac{F_4 c^2}{6El}(c+l)$

The total integrated deflection is calculated by summing the resultant deflection from all three forces evaluated.

$$y_{max} = y_{uniform} + y_{F_3} + y_{F_4}$$

The final design achieves a maximum deflection of $y_{max} = 4.9\ \mu m$, which satisfies the stiffness requirement of $y_{max} \leq 5\ \mu m$.

Linear rail and carriage mounting arrangement

Manufacturing

The Y-stage plate and axis plate are manufactured from Aluminium 6063-T6 using CNC machining. Primary datum faces are established initially to control straightness, flatness and parallelism, and are used as references for machining the linear rail, lead screw and encoder interfaces.

Rail mounting faces are machined in a single setup to ensure accurate alignment and minimise bearing preload. All fastener holes are drilled and tapped relative to the established datums, followed by deburring and chamfering to improve assembly quality.

Design Evolution

Early iterations of the Y-axis plate focused on increasing plate thickness to act against the loads transmitted from the Z-stage and workpiece. While this approach successfully reduced elastic deflection, it resulted in unnecessary mass and inefficient material usage, which adversely affected dynamic performance.

To improve stiffness efficiency, the design was revised to increase the plate width rather than thickness. This modification significantly increased the second moment of area, providing a more effective reduction in bending deflection with a minimal increase in mass. As a result, the plate thickness could be reduced while satisfying the stiffness requirement.

The final design achieves a maximum calculated deflection of $4.9\ \mu m$, which meets the specified limit of less than $5\ \mu m$, while minimising mass with improved structural efficiency. This iterative design process resulted in a balanced solution that satisfies stiffness, weight and manufacturability requirements.

Final Design Description

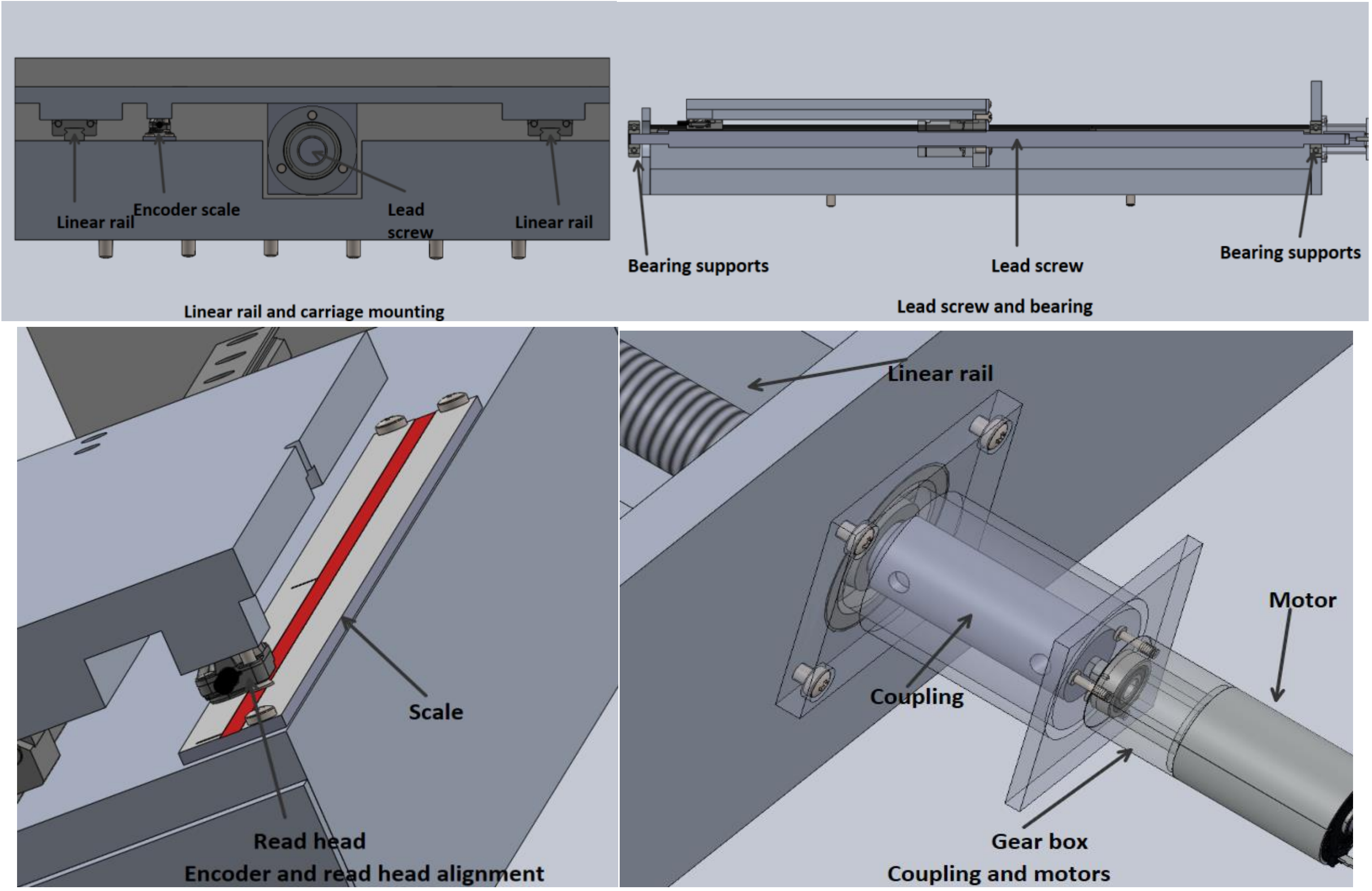

Figures 9,10,11,12 (Clockwise)- Details of mounting assembly of Y stage

1.3. The X Stage

Function

The function of the X stage is the x-axis translation of the disc being manufactured as well as all the previously discussed components. This means it bears the loads and moment induced by all previous stages and components, and load ratings for all moving parts are the highest out of the assembly. The linear bearings on the x stage moving platform will have to withstand the weight of the y axis and x moving platform, as well the moments induced by the linear bearings of the y moving stage and everything mounted on it. It must provide a linear horizontal translation of 600mm, including the width of the moving platform. As there is a lesser concern of deflection than for the previous stages, dimensions such as width and thickness can be relatively minimized to decrease costs.

Service Conditions

The X-stage supports the entire Z and Y stage assemblies, as well as the weight of its own moving carriage. Therefore, it experiences the vertical loading of the reaction forces to F3 and F4 from the Y axis linear bearings and the combined loads of the Y stage and the X axis moving plate. The resultant forces on the X axis bearings are dependent on the spacing between them, which is constrained by the width of the X axis stage, as well as the spacing of the Y axis bearings, which is fixed. The resultant loads acting on a single recirculating bearing carriage is half the load found on the 2D FBD used for analysis. *See Appendix E.1 for calculations.* Although the stage has been deemed stable for its application, the X stage could be strapped down for further stability.

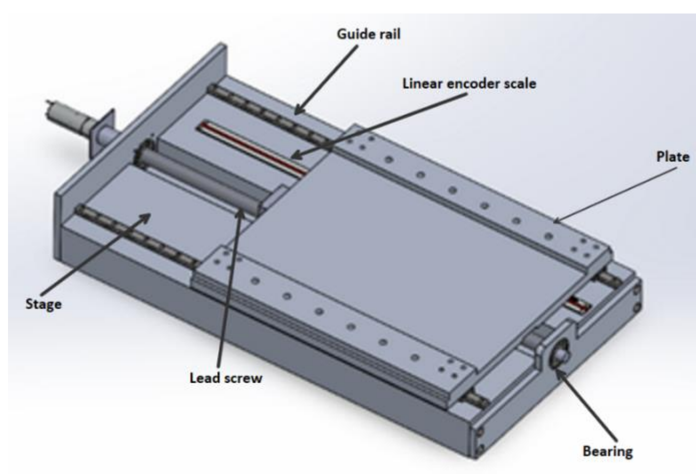

Figure 13- Labelled components of X axis assembly

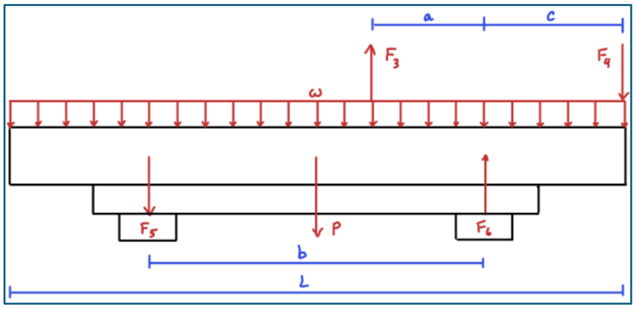

Figure 14- Dimensions and FBD of X stage (front view)

Free Body Diagram

- $F_5 = 363.99\ N$
- $F_6 = 852.29N$

Chosen Embodiment

- **Linear Guides:** NSK PU12UR recirculating linear rails with 4 carriages
- **Lead Screw:** Trapezoidal lead screw; SRA 5-20x4M (Ø15 mm, 20 mm lead)
- **Nut:** XCB7500 anti-backlash nut
- **Support Bearings:** 6302 deep-groove ball bearings
- **Drive:** Maxon DCX 26L GB KL 24V DC motor with GPX 26 A planetary gearbox (5.3:1)
- **Position Feedback:** Linear optical encoder

Linear Guide Rails Selection

Based on the geometric and load constraints, the linear rails chosen were the PU12UR series from the NSK catalog. They were selected because they are rated for 4000N, which covers the maximum load on a bearing, F6 times the safety factor of 4 (or 3409.2N), and have a maximum length of 800mm, covering the 600mm of movement and added lengths of moving stages, stoppers and bearings required for the X stage. *See Appendix E.2 for guide rail selection calculations.*

Other linear guides were considered, such as those listed in the PE series, which offered similar characteristics in travel length and load bearing abilities. However, the NSK website lists the PU series as more precise, so we chose to select the PU guide rail that most fit our requirements. The PU12UR is the higher rated of the 800mm series, but in not venturing into 1000mm long guide rail options we expect to save on unnecessary costs, since the loads are still accounted for.

Lead Screw and Nut Selection

Lead Screw Selection

The maximum axial load on the lead screw is dependent on the acceleration required to make the plate (and all of the axes atop it) travel the 600mm distance in 3 seconds, with 0.5s of acceleration and decelerations available. The force against the screw with safety factor of 4 is 215.6N.
(*See E.1 and E.3 for calculations.)*

Through iteration on Excel, the torque and rpm formulas were used to select a leadscrew with a torque and rpm that did not surpass the allowed values on the Thomson catalog (*see Appendix E.4 for iterations*). Using this method, we have selected the leadscrew 5-20x4M, as it can comfortably be subject to 225.77Nm (903.08Nm with safety factor) of torque and 720rpm of rotational speed (*Appendix E.3*). This also ensures a minor diameter large enough to fit a bearing that can take the loads we expect.

Nut selection

The bearing nut chosen is the XCB7500 model from the Thomson catalog, which is preloaded and amply rated for the expected axial load of 53.9N. Its 20mm threaded diameter is additionally compatible with our chosen leadscrew. Other nuts either did not have the required diameter or were not preloaded.

Bearing Selection

We have selected the ball bearings to fit the second mounting configuration shown in the Thomson catalog as the loads are not overly high, and as such are to be two identical deep groove ball bearings. Assuming a worst-case scenario in which all the load falls on one bearing, and multiplying by a safety factor of 4, the 6302 bearing has been chosen, as it is the smallest that can withstand 4406.8N of radial force. Axial force has been neglected, as the radial force dominates by the equivalent dynamic bearing load formula. The bearing life calculations for 90% efficiency rate this application at 2800 hours. (*Appendix E*)

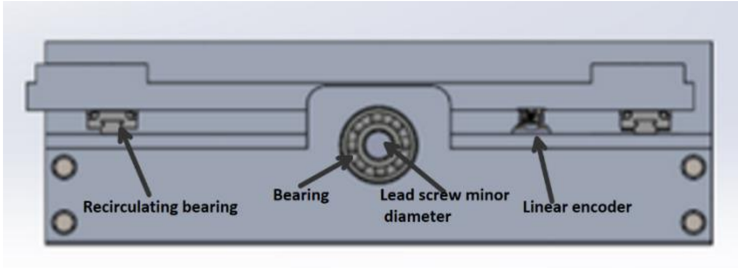

Figure 16- Bearing mounting on X axis bearing mount

Motor Selection

The motor has been chosen iteratively as well, by verifying that the allowable gearbox ratio combinations reached the required torque transmission while not exceeding the maximum permissible rpm of the leadscrew. The necessary torque-angular velocity combinations were then checked on a T-w diagram to ensure they were within range of the motor. In this way, the motor DCX26L GB KL 24V was selected, coupled with the gearbox GPX26A 5.3:1. Accounting for the gearbox efficiency of 0.9, the combination fit all the requirements for rpm and torque while remaining one of the cheaper options. (Appendix E)

Design Evolution

The dimensions of the X stage largely remained constant due to an initial decision to keep a standardized width throughout the axis stages. Due to this, and the geometric constraints imposed by the Y axis in the FBD analysis, the X-plate and its bearing's dimensions and spacings also remained mostly fixed throughout the design process. This meant that there was a semi-fixed set of values to use as a benchmark for those components that could be iterated.

The X-stage leadscrew was iterated as illustrated in E.4 under various constraints, notably keeping the rpm within 80% of the maximum rotational speed as dictated by the catalog and keeping the minor diameter within range of what the required load-rated ball bearings could be mounted on. The latter is dependant on the weight of the Y and Z axes, which changed at several stages by up to 800N due to iterations on the Y stage dimensions, prompting several rounds of leadscrew selection to satisfy the critical speed and buckling constraints.

The motor selection also underwent several variations, as multiple combinations of torques, gearboxes and voltages were tried at various stages as the weight loads from the axes changed. High torque and low gearbox ratio combinations were tried (89.4Nm and 3.9:1, for one), but they were found to overshoot the required torque unnecessarily while grazing the rpm threshold, so the final combination was chosen to balance the two.

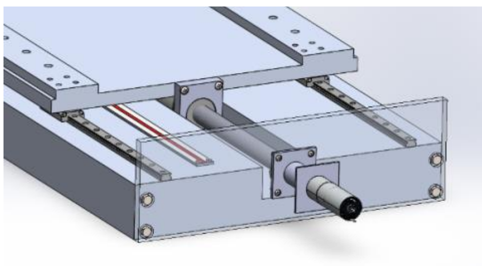

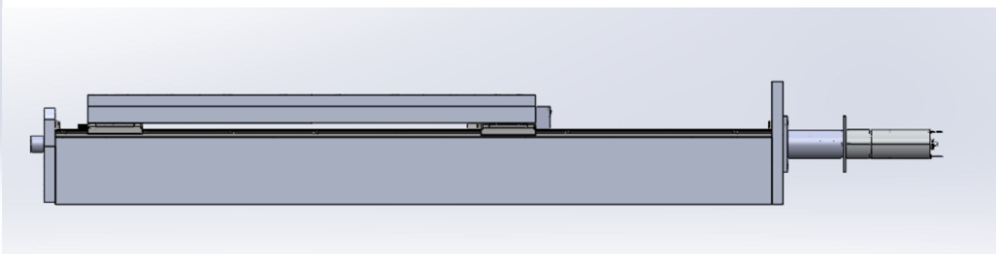

Figure 17,18- Varying views of X stage

Group Work Reflection

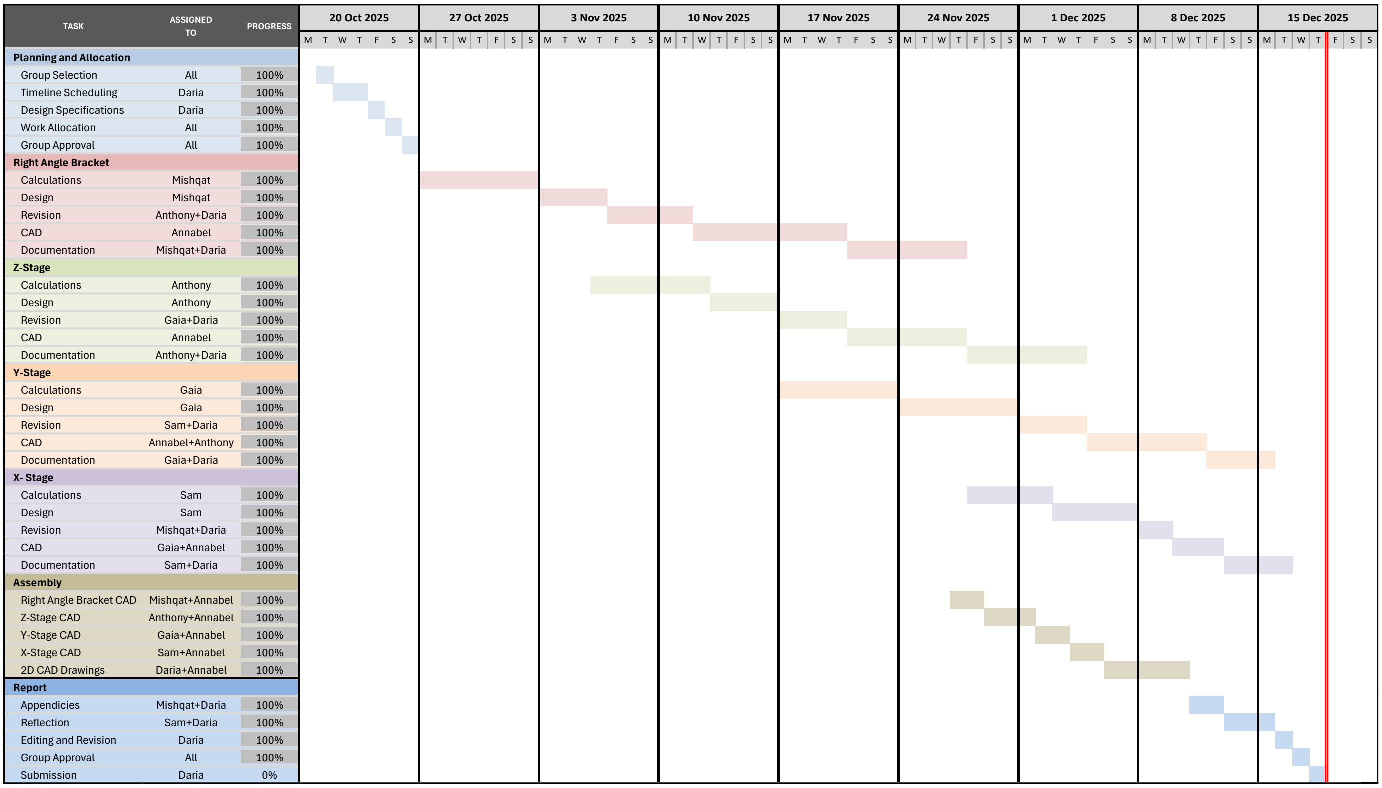

Figure 19- Gantt chart of group progress

Initial Plan

The initial plan was to establish a shared technical foundation by completing
Once the L stage was completed, the CS team would move on to the X stage, while the other teams continued working on the current stage. This approach ensured that there was always productive work being done. After completing the first full pass of all stages, teams were reassigned to review the work and implement any required changes. Each subsequent pass took less time as the design matured. By the third pass, the entire team reviewed each stage briefly to ensure that everyone had contributed to every part of the project.

Assignments and Reassignments

A Gantt chart was used to allocate tasks and manage deadlines across all sub-teams. Individual strengths were considered, as some members were more skilled in CAD, calculations, or writing. During certain stages, members were allowed to switch teams to maximise efficiency. However, one person from each team was required to remain in place during a pass to ensure continuity and to support any new members joining the team.

For example, during motor selection for the Z stage, a member from the CAD team had strong experience using the Maxon Motors website. This knowledge was shared with their teammate, who could then carry that experience forward into later stages. Although this process slightly slowed the schedule, it was considered beneficial as team members learned while completing real tasks rather than through separate training time.

Identified using a team role

A Belbin team roles test was carried out to identify individual strengths within the group. The roles identified included Resource Investigator, Co-ordinator, Specialist, Monitor-Evaluator, Implementer, and Completer-Finisher. These roles helped guide task allocation. For example, the Completer-Finisher was always involved during the final pass, while the Co-ordinator handled room bookings and meeting schedules.

Conflict Management

The use of the Gantt chart made it easy to track progress and identify uneven contributions early. When this occurred, team members were asked to provide a valid reason. If no reasonable explanation was given, they were expected to dedicate additional personal time to complete their assigned tasks.

One example involved a team member missing a meeting due to an unforeseen external commitment, which was considered acceptable. However, in cases such as oversleeping, the individual was required to make up the lost time independently. This system was well received by the team and helped maintain accountability.

Reflection

A key reflection shared across the team was the importance of avoiding procrastination, as delaying work significantly increased stress towards the end of the project. Another reflection was the value of maintaining a positive attitude. A supportive and relaxed atmosphere helped improve morale and made collaboration easier for everyone.

Change

The main change to the original plan was an extension of the time allocated to each task. This led to a significant workload near the end of the project, leaving sufficient time for only one final design pass instead of the planned multiple.

Appendix A

Task 2: 2D CAD Drawings

See PDF Drawings that follow.

Figure A.1- Assembly CAD Drawing of Model

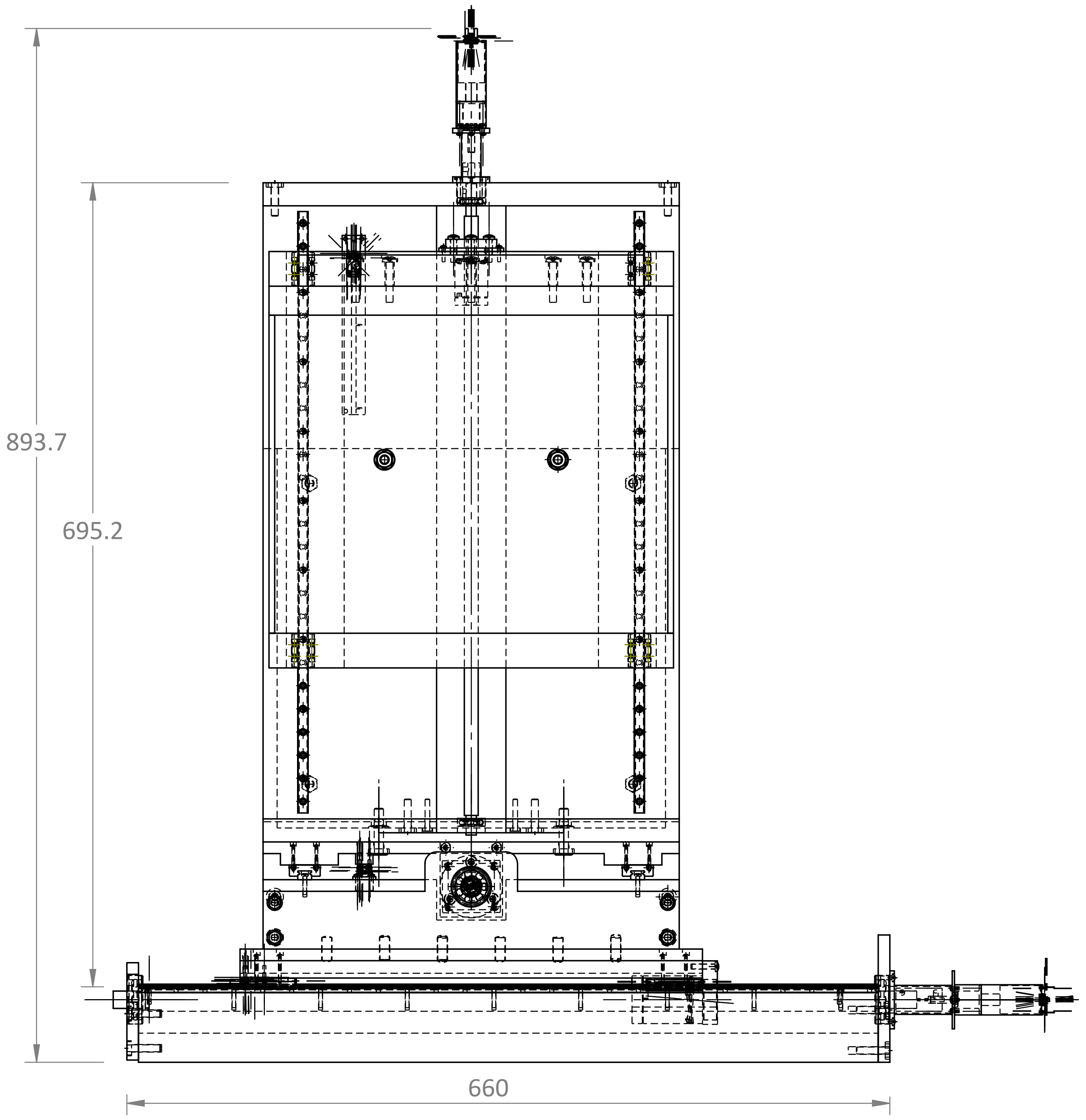

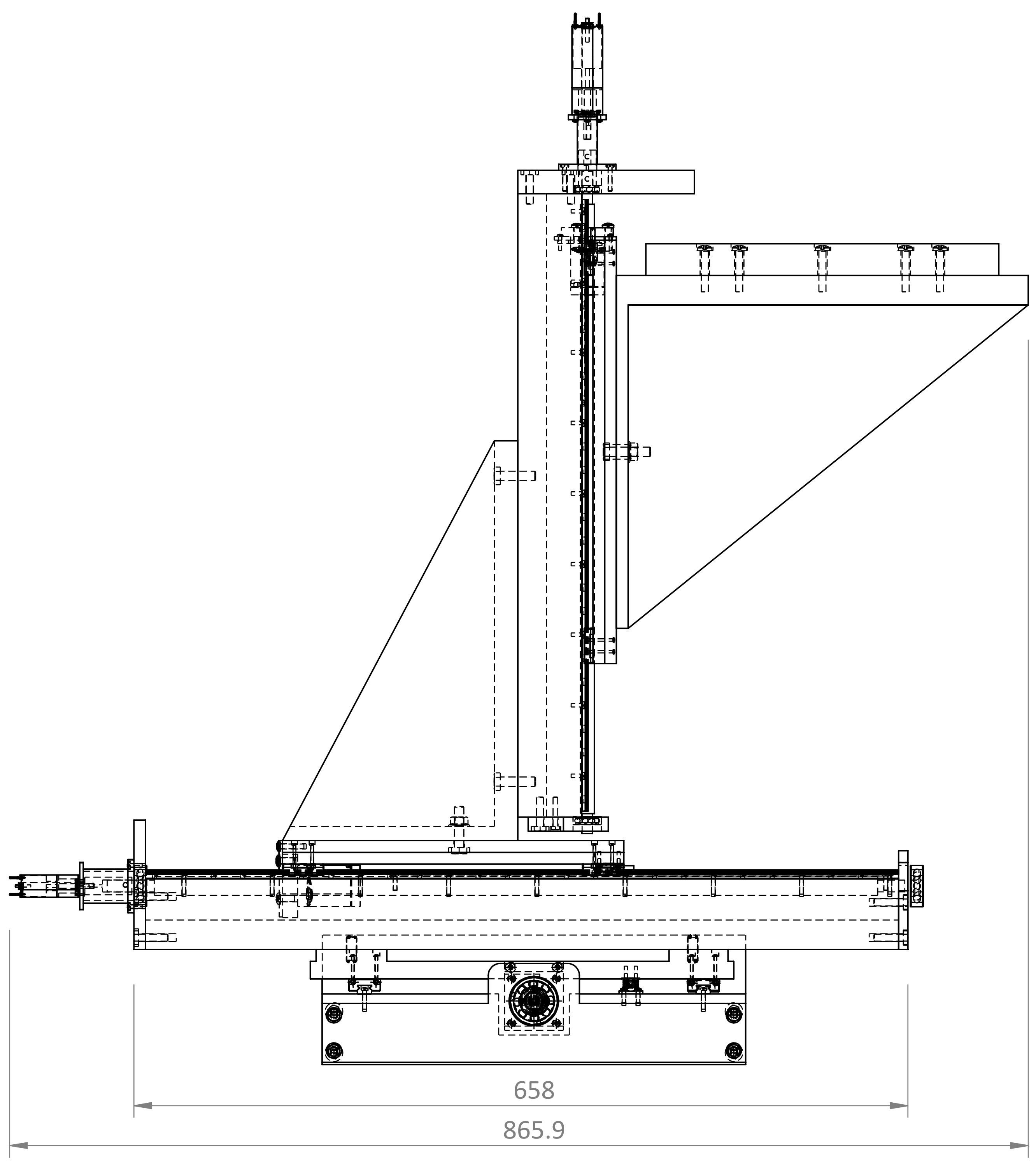

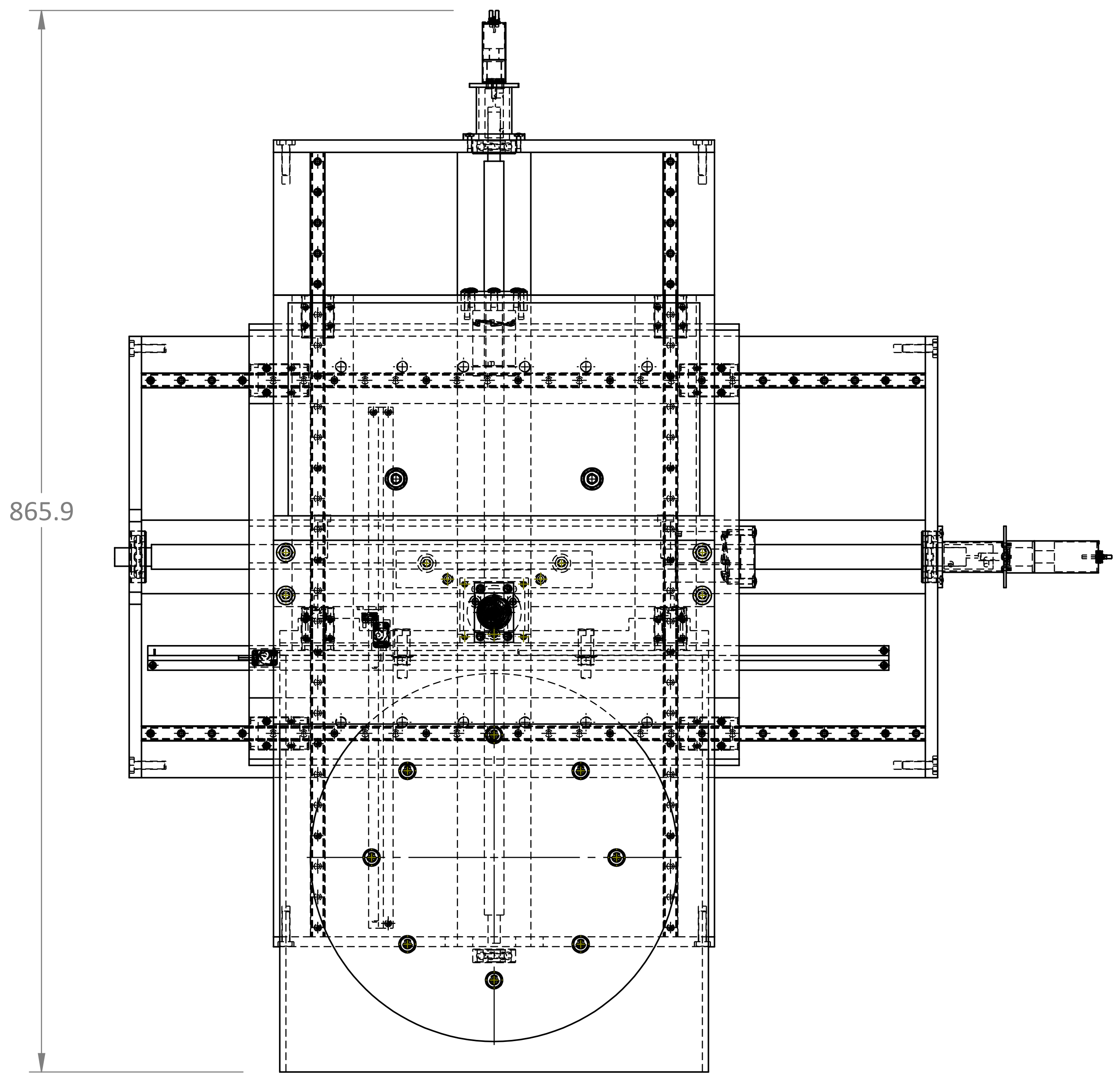

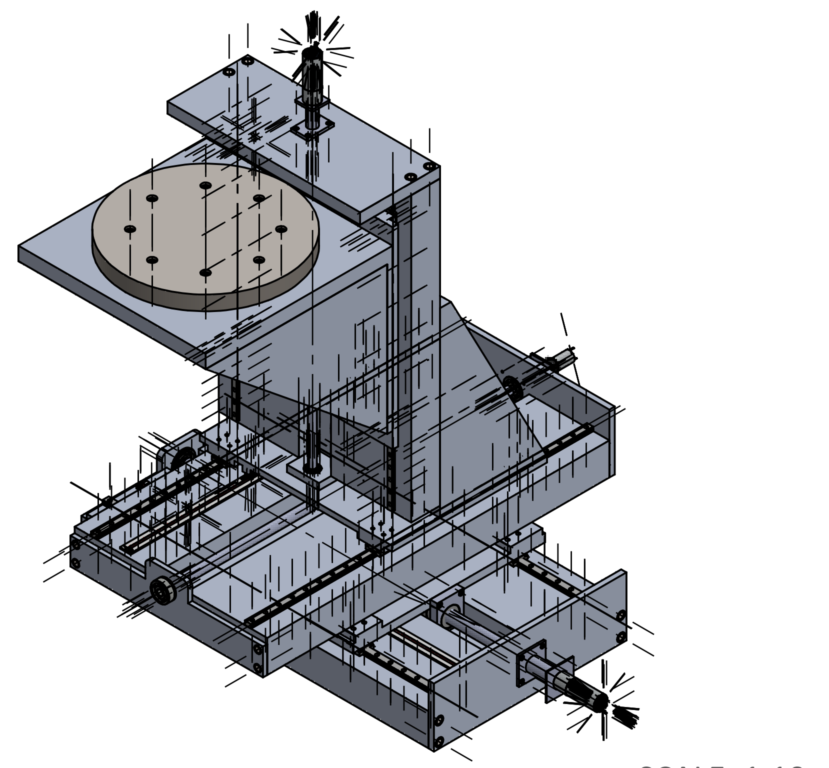

SCALE: 1:10

First Angle

Department of Mechanical, Aerospace & Civil Engineering
UNIVERSITY OF MANCHESTER
MACE

Mat'l: N/A	No. Req'd: 1	DO NOT SCALE DRAWING	Dimensions in millimeters
Drawn by: ANNABEL LEE		Dwg Title: Full Assembly Drawing	
Student No. 11509538			
Contact no: +447848938155		Dwg No: Dwg No	SHEET 1 of 1 — A2
Email: annabel.lee@student.manchester.ac.uk			
Date: Thursday, December 18, 2025	SCALE:		File: Full Assembly Drawing

ITEM NO.	PART NUMBER	QTY.
1	Right Angled Bracket	1
2	Rib	2
3	Circular Platform	1
4	Z-axis Plate	1
5	XCF5000 nut	1
6	Z Column	1
7	PU09TR_rail	2
8	PU09TR_slider	4
9	Z-axis Stopper	1
10	Motor	1
11	Couple	1
12	Y-axis bracket	1
13	bearing mount bottom	1
14	NSK_609	2
15	Y-axis Plate	1
16	Y-baseplate	1
17	Plate for Lead Nut	1
18	X-axis stage	1
19	PU12TR_640_rail	2
20	PU12TR_slider	4
21	X-axis plate	1
22	PU12UR_slider	4
23	PU12UR_rail	2
24	Y-axis Stopper	1
25	X-axis Stopper	1
26	z-stage motor mount	1
27	Y-axis Motor.stp	1
28	NSK_6300	2
29	ISO 4015 - M4 x 25 x 14-N	2
30	ISO 4015 - M6 x 25 x 18-N	22
31	ISO 4015 - M3 x 20 x 12-N	4
32	ISO 4015 - M8 x 30 x 22-N	4
33	ISO 4015 - M8 x 35 x 22-N	4
34	ISO 7045 - M3 x 10 - Z - 10N	29
35	ISO 7045 - M2.5 x 8 - Z - 8N	4
36	ISO 7045 - M2 x 20 - Z - 20N	48
37	ISO 7045 - M6 x 35 - Z - 35N	8
38	ISO 7045 - M4 x 20 - Z - 20N	4
39	ISO 7045 - M5 x 12 - Z - 12N	3
40	ISO 7045 - M3 x 16 - Z - 16N	36
41	ISO 7045 - M3 x 12 - Z - 12N	3
42	ISO 7045 - M2.5 x 3 - Z - 3N	4
43	ISO 7045 - M2.5 x 12 - Z - 12N	4
44	ISO 7045 - M5 x 20 - Z - 20N	3
45	NSK_6302	2
46	ISO - 4161 - M8 - N	4
47	ISO 2339 - A - 8 x 22 - St	12
48	ISO 7046-1 - M2.5 x 12 - Z - 12N	6
49	CR-PHMS 0.06-80x0.25x0.25-N	3
50	X-axis Motor.stp	1
51	Y lead screw	1
52	X lead screw	1
53	Part1^NEW ASSEMBLY	1
54	Y stage bearing mount	1
55	X-axis bearing mount	1
56	Z Lead screw	1
57	Y-axis Couple	1
58	Y-axis motor mount	1
59	X-axis Couple	1
60	X-axis motor mount	1
61	L155 Z stage encoder	1
62	Linear Encoder Head	3
63	L425 Y stage encoder_new	1
64	L605 X stage encoder	1
65	XCF6200 nut	1
66	Y plate for lead nut	1
67	XCB7500 nut	1
68	X plate for lead nut	1

Figure A.2- Second Drawing of Exploded View of Model

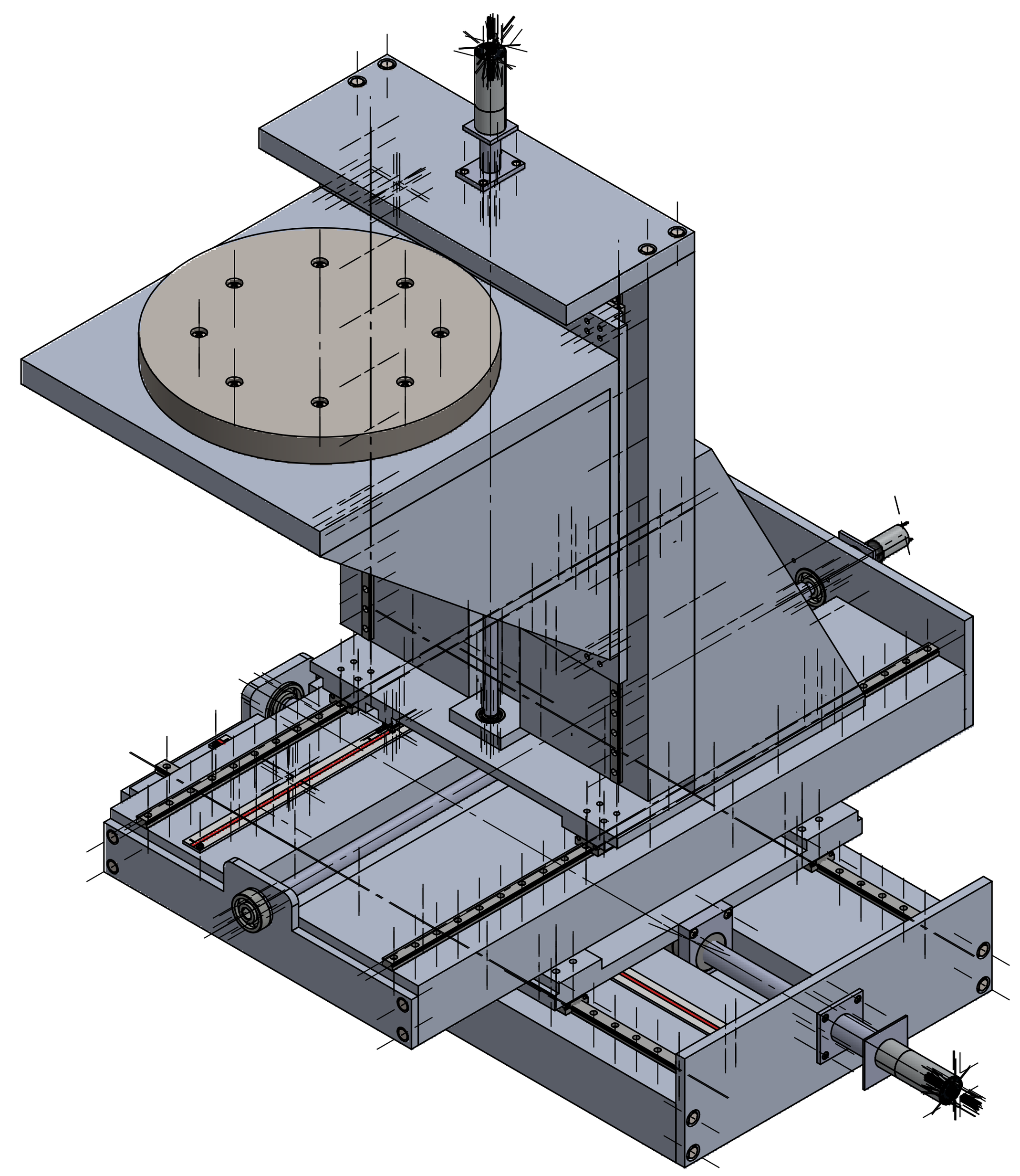

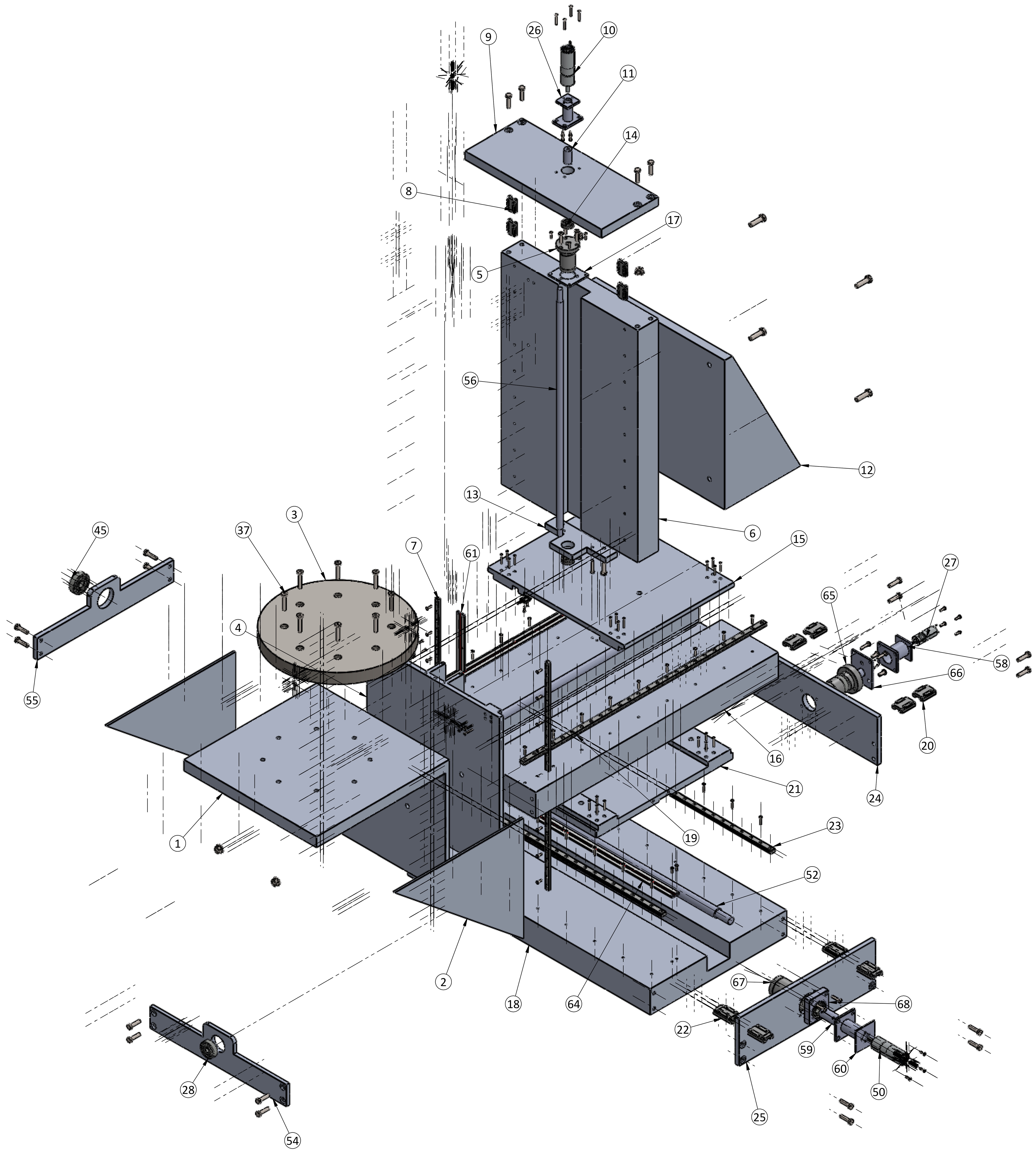

First Angle

Department of Mechanical, Aerospace & Civil Engineering
UNIVERSITY OF MANCHESTER
MACE

Mat'l: N/A | No. Req'd: 1

Drawn by: ANNABEL
Student No: 11509538
Contact no: +447848938155
Email: annabel.lee@student.manchester.ac.uk

Date: Thursday, December 18, 2025

DO NOT SCALE DRAWING | Dimensions in millimeters

Dwg Title: Exploded View

Dwg No: Dwg No

SHEET 1 of 1 | A1

File: MACE A1

Figure A.3.1- Z-Stage Baseplate

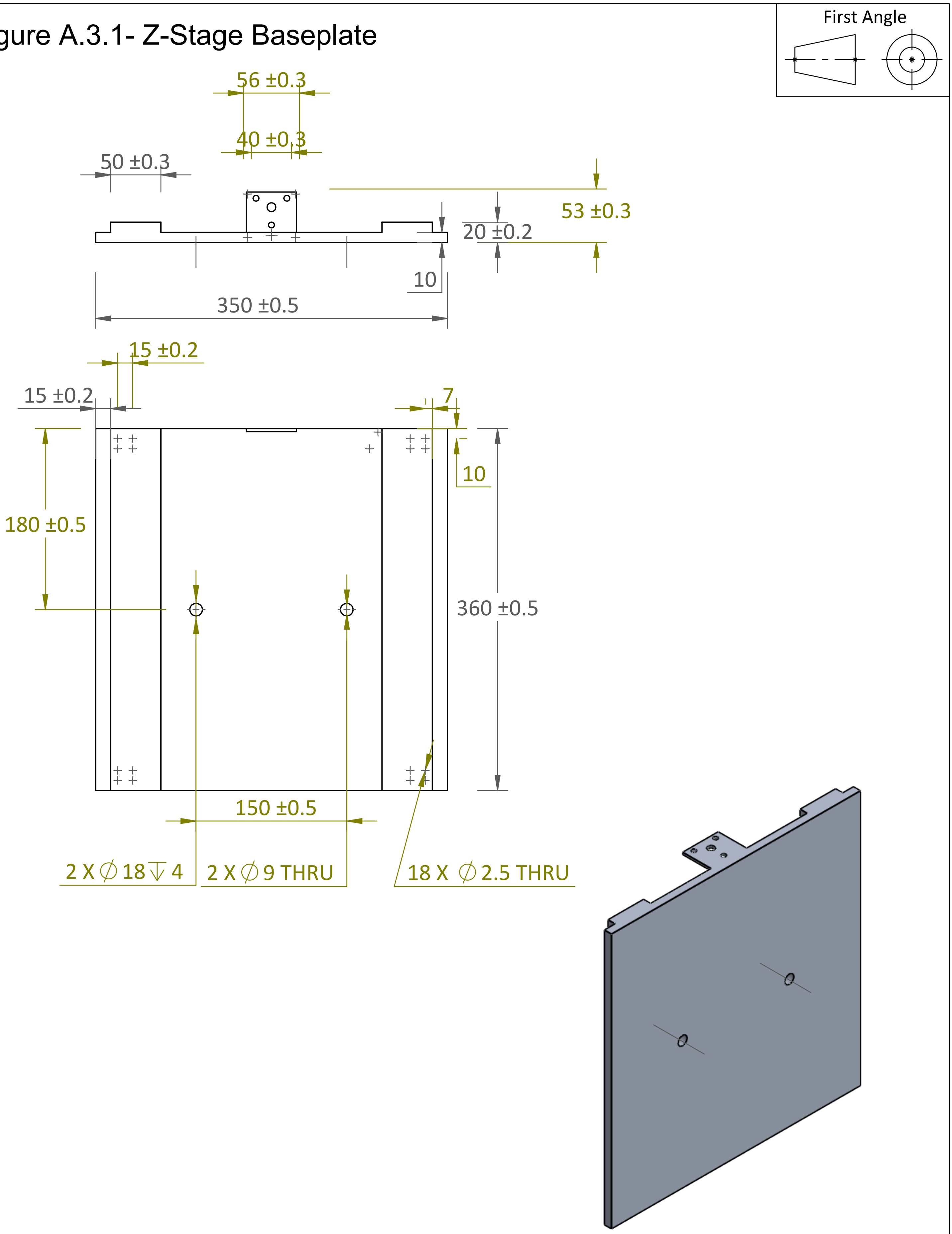

Department of Mechanical, Aerospace & Civil Engineering
UNIVERSITY OF MANCHESTER
MACE

Mat'l: ALUMINIUM	No. Req'd: 1	DO NOT SCALE DRAWING	Dimensions in millimeters
Drawn by: AHMED MISHQAT		Dwg Title: **Z-Plate**	
Student No. 11550212			
Contact no: N/A			
Email: ahmed.mishqat@student.manchester.ac.uk		Dwg No: Dwg No	SHEET 1 of 1 — A4
Date: Thursday, December 18, 2025	SCALE 1:2		File: Z-Plate_D

Figure A.3.2- Z-Stage Column

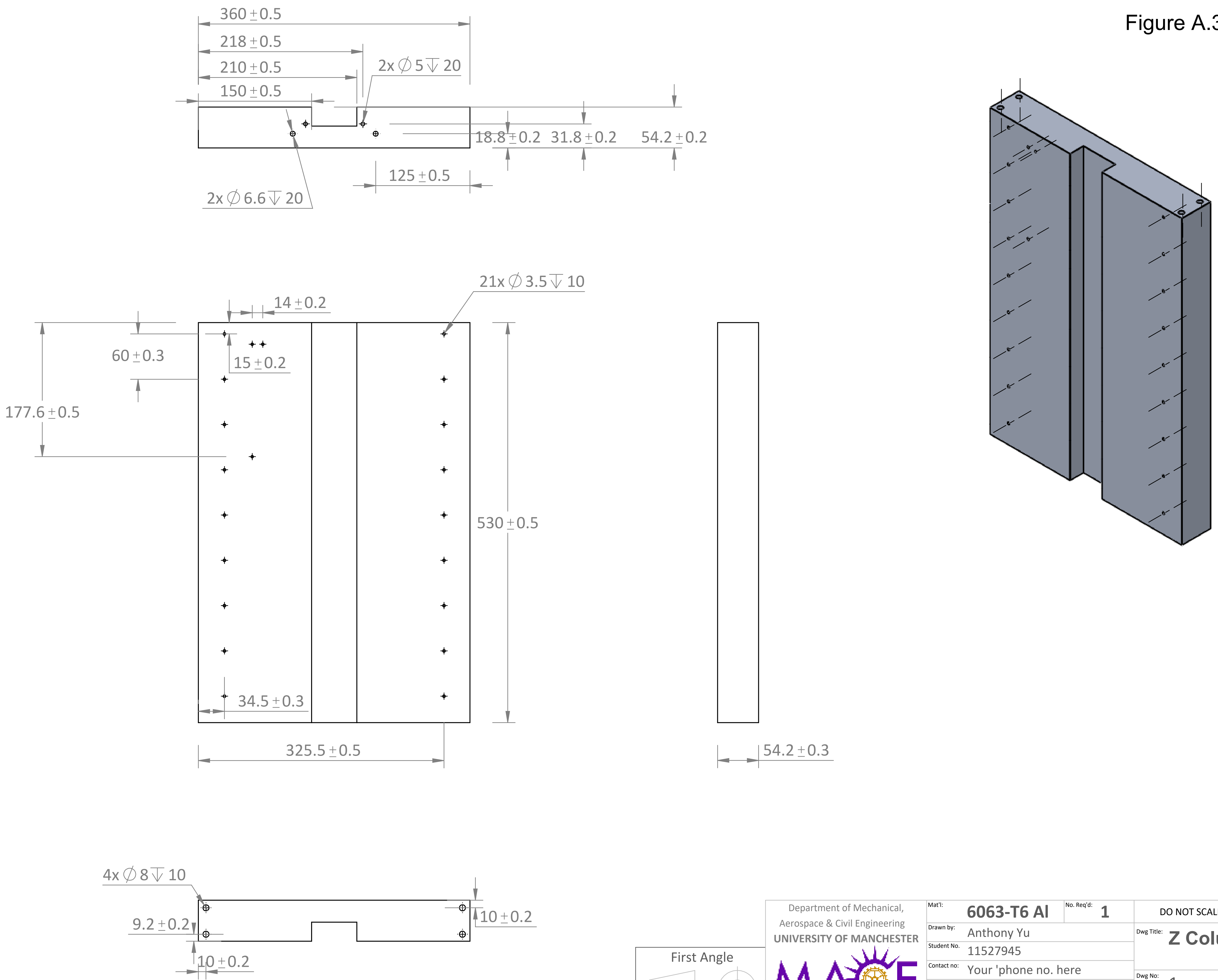

First Angle

Department of Mechanical, Aerospace & Civil Engineering
UNIVERSITY OF MANCHESTER

Mat'l: 6063-T6 Al	No. Req'd: 1	DO NOT SCALE DRAWING	Dimensions in millimeters
Drawn by: Anthony Yu		Dwg Title: **Z Column**	
Student No. 11527945			
Contact no: Your 'phone no. here			
Email: anthony.yu@student.manchester.ac.uk		Dwg No: 1	SHEET 1 of 1 / A3
Date: 18 December 2025	SCALE: 1:10	File: Z-Columns	

Figure A.3.3- Z-Stage L Bracket

First Angle

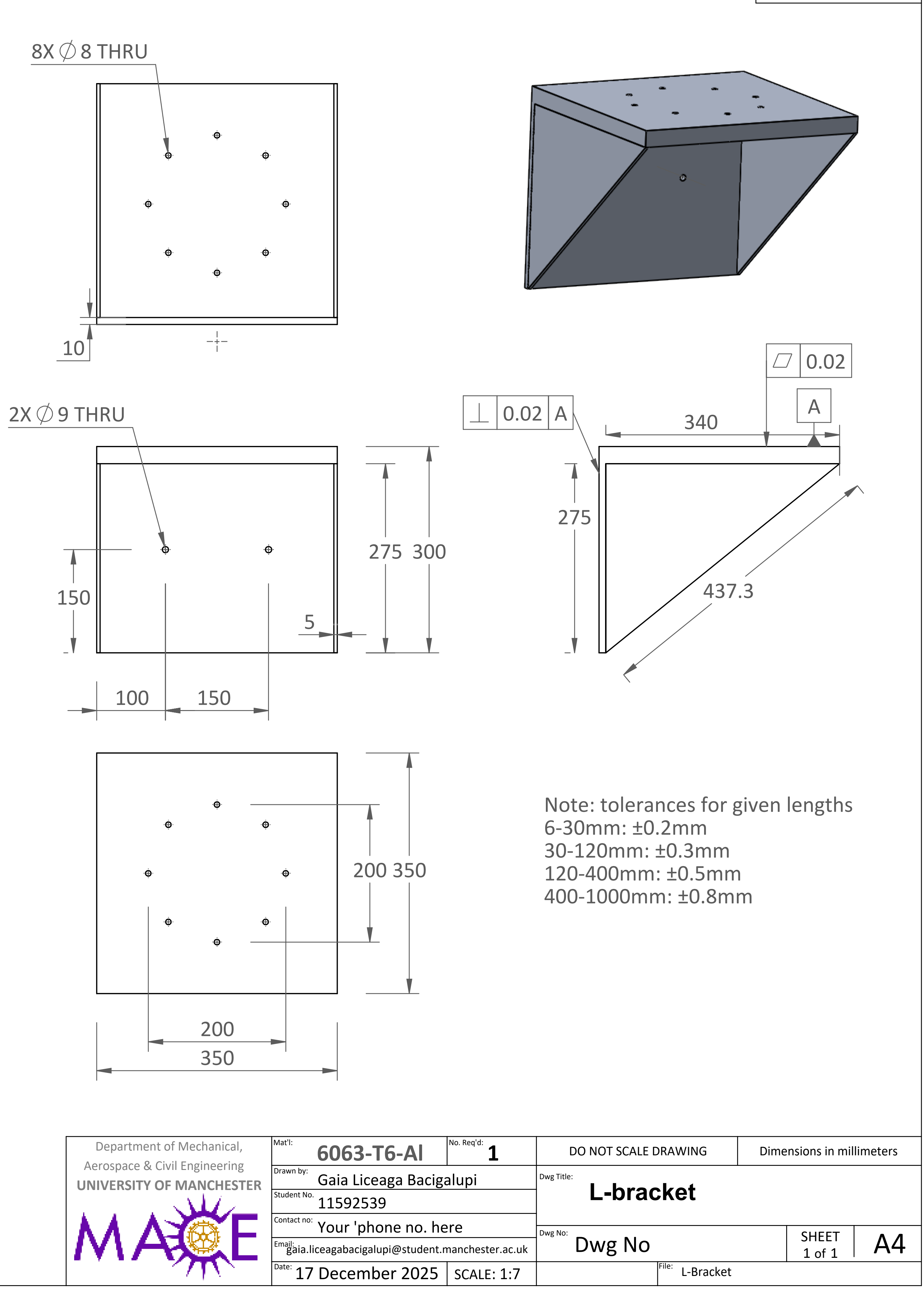

First Angle

Figure A.4- Y-Stage

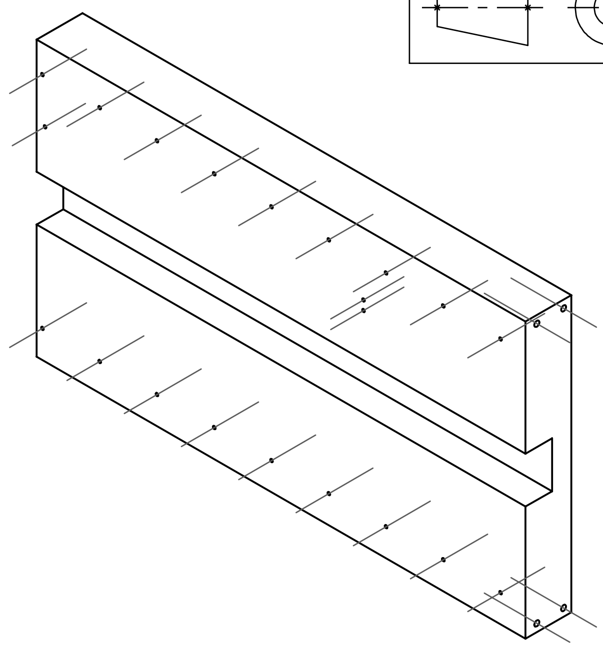

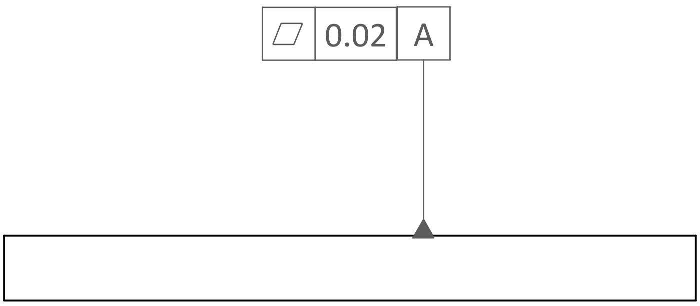

Tolerance
3-6mm = 0.1
6-30mm = 0.2
30-120mm = 0.3
120-> = 0.4

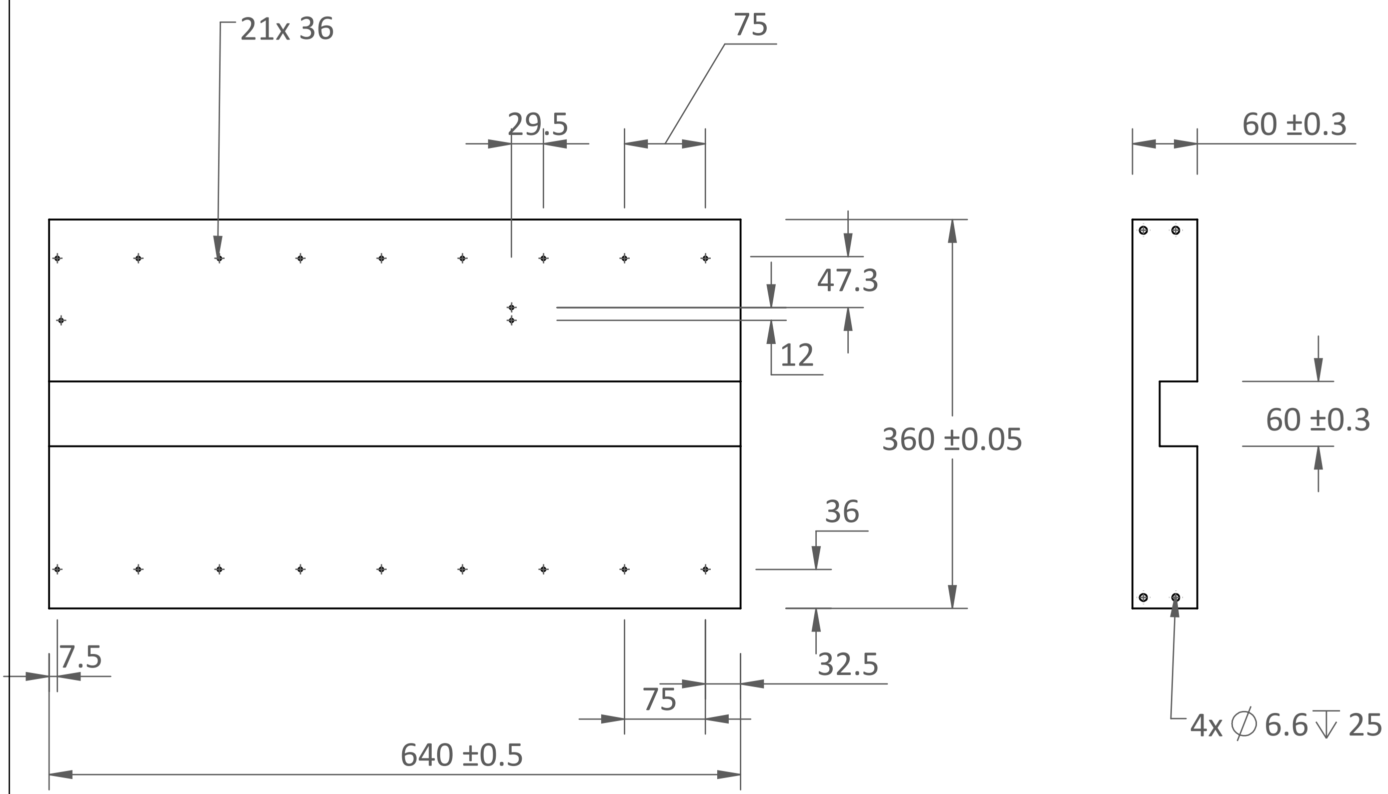

Department of Mechanical, Aerospace & Civil Engineering UNIVERSITY OF MANCHESTER MACE	Mat'l: Aluminium 6063-T6	No. Req'd: 01	DO NOT SCALE DRAWING	Dimensions in millimeters
	Drawn by: Samuel Ahiwe		Dwg Title: **Y Stage**	
	Student No. 11527747			
	Contact no: +447598445209		Dwg No: 01	SHEET 1 of 1 · A4
	Email: samuel.ahiwe@student.manchester.ac.uk			
	Date: 18 December 2025	SCALE: 1:10	File: MACE A4 Po - Copy	

Figure A.4.1- Y Moving Plate

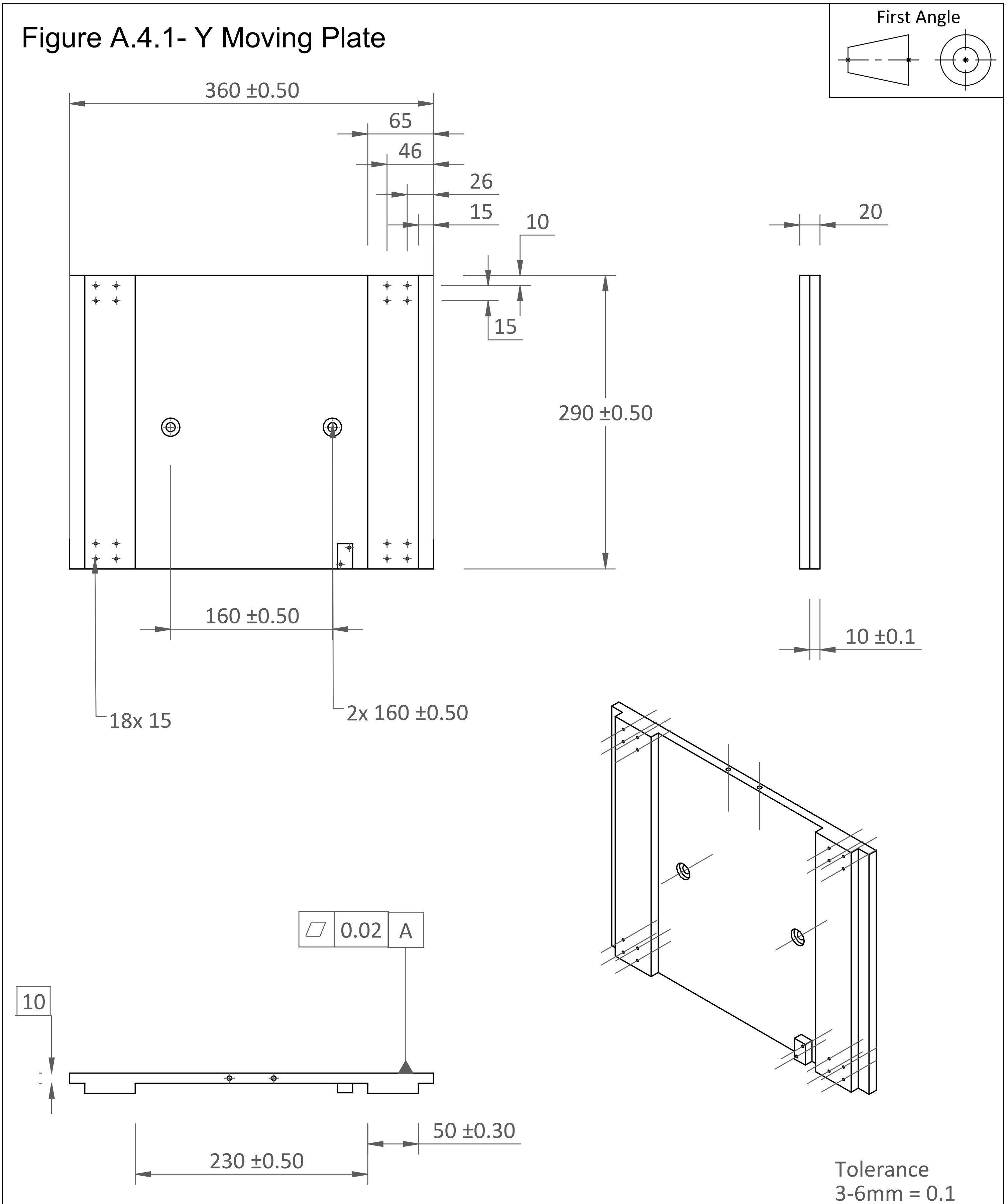

Tolerance
3-6mm = 0.1
6-30mm = 0.2
30-120mm = 0.3
120-> = 0.5

Department of Mechanical,
Aerospace & Civil Engineering
UNIVERSITY OF MANCHESTER
MACE

Mat'l: Aluminium 6063-T6
No. Req'd: 1
DO NOT SCALE DRAWING
Dimensions in millimeters

Drawn by: Samuel Ahiwe
Student No. 11527747
Contact no: +447598445209
Email: samuel.ahiwe@student.machester.ac.uk

Dwg Title: Y plate
Dwg No: 01
SHEET 1 of 1
A4
Date: 18 December 2025
SCALE: 1:5
File: Y stuff

Figure A.5.1- X Moving Plate

First Angle

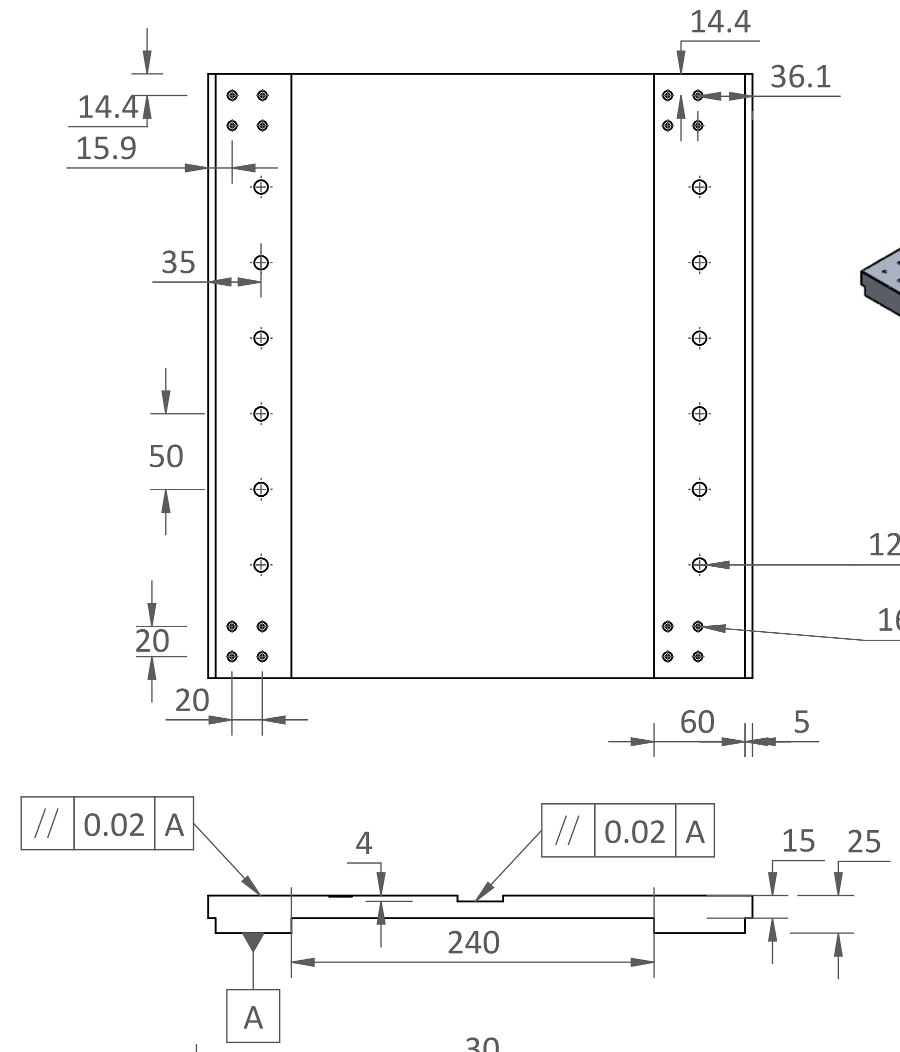

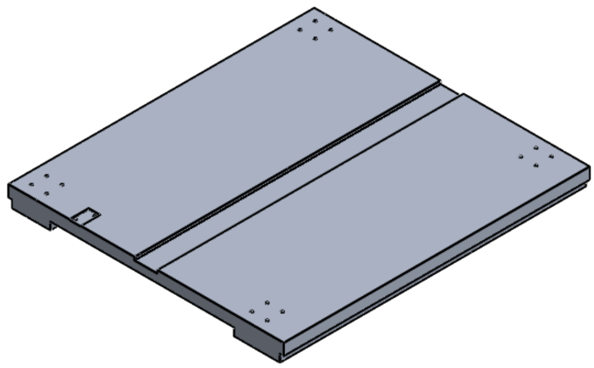

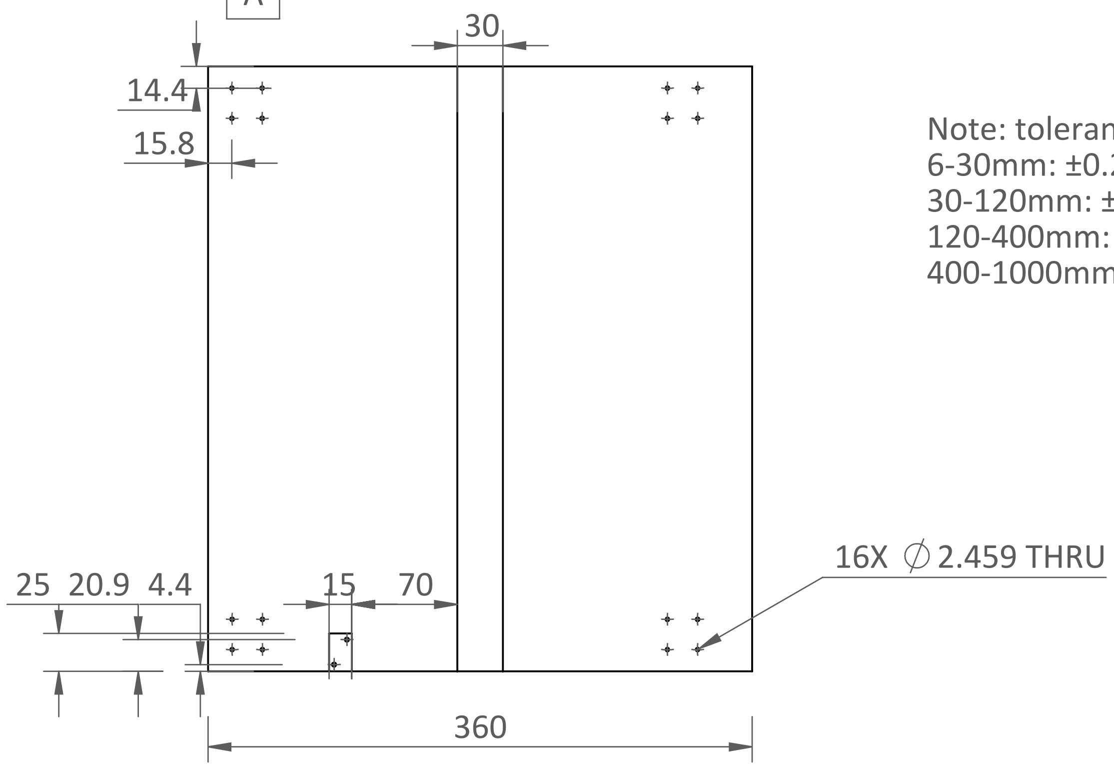

Note: tolerances for given lengths
6-30mm: ±0.2mm
30-120mm: ±0.3mm
120-400mm: ±0.5mm
400-1000mm: ±0.8mm

Department of Mechanical, Aerospace & Civil Engineering
UNIVERSITY OF MANCHESTER
MACE

Mat'l: **6063-T6 Al**
No. Req'd: **1**
DO NOT SCALE DRAWING
Dimensions in millimeters

Drawn by: Gaia Liceaga Bacigalupi
Student No. 11592539
Contact no: Your 'phone no. here
Email: gaia.liceagabacigalupi@student.manchester.ac.uk

Dwg Title: **X Moving Plate**
Dwg No: Dwg No
SHEET 1 of 1
A4
Date: 18 December 2025
SCALE: 1:5
File: XMovingplate

Figure A.5.2- X-Stage

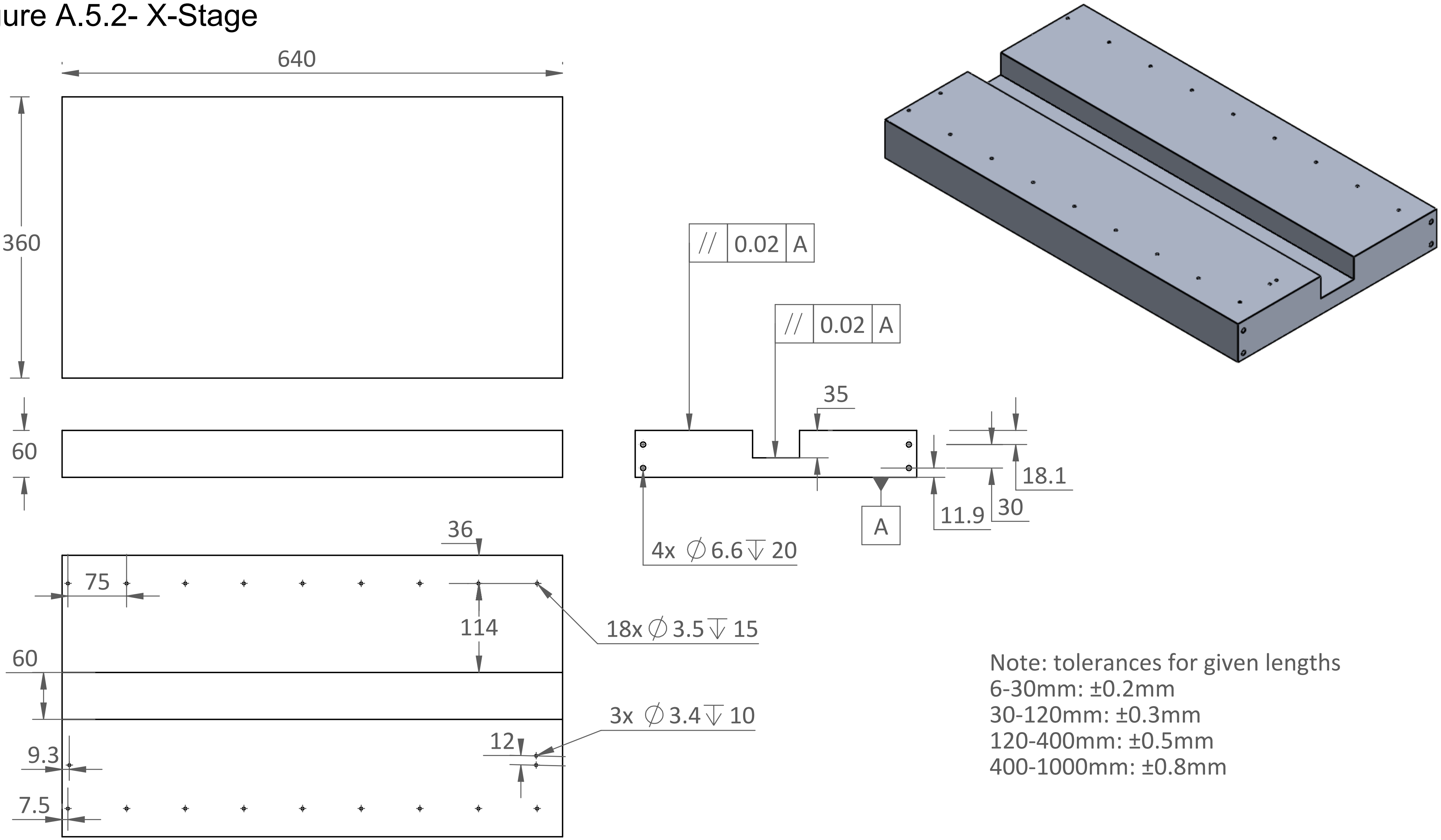

Note: tolerances for given lengths
6-30mm: ±0.2mm
30-120mm: ±0.3mm
120-400mm: ±0.5mm
400-1000mm: ±0.8mm

First Angle

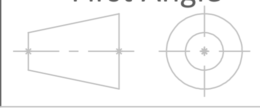

Department of Mechanical, Aerospace & Civil Engineering
UNIVERSITY OF MANCHESTER
MACE

Mat'l: 6063-T6 Al	No. Req'd: 1	DO NOT SCALE DRAWING	Dimensions in millimeters
Drawn by: Gaia Liceaga Bacigalupi		Dwg Title: X-Axis Stage	
Student No. 11592539	Mech		
Contact no: Your 'phone no. here		Dwg No: Dwg No	SHEET 1 of 1 — A4
Email: gaia.liceagabacigalupi@student.manchester.ac.uk			
Date: 18 December 2025	SCALE: 1:7	File: DesignXStage1	

Appendix B – Right Angle Bracket

MATERIAL	CATEGORY	DENSITY (g/cm^3)	YIELD STRENGTH (MPa)	ELASTIC MODULUS (GPa)
1050-H14	Aluminium	2.71	70	69.0
2024-T3	Aluminium	2.78	345	73.0
5052-H32	Aluminium	2.68	193	70.0
6061-T6	Aluminium	2.70	255	68.9
6082-T6	Aluminium	2.70	250	69.0
6063-T6	Aluminium	2.70	214	68.9
7075-T6	Aluminium	2.81	470	71.0
7475-T61	Aluminium	2.80	460	72.0
MILD (S275)	Steel	7.80	250	210
HIGH STRENGTH (EN8)	Steel	7.83	500	210
4130 CHROMOLY	Steel	7.85	460	205
4340 ALLOY	Steel	7.85	710	190
304 STAINLESS	Steel	8.00	215	193
316 STAINLESS	Steel	7.99	290	193

Figure B.1 – Material properties of common aluminium and steel alloys

MATERIAL	COST $(£/kg)$	MACHINING	NOTES	SCORE
2024-T3 Al	4.5	2	Good; observe corrosion	9.0
5052-H32 AL	2.8	2	Good; soft	5.6
6061-T6 Al	3.0	1	Excellent	3.0
6063-T6 Al	2.7	1	Excellent; extrudable	2.7
6082-T6 Al	3.2	2	Good	6.4
7075-T6 Al	5.0	2	Good; not weldable	10.0
7475-T61 Al	5.5	3	Tough	16.5
4130 CHROMOLY STEEL	3.0	3	Tough	9

Figure B.2 – Decision Matrix for Material Selection

Lowest Score = 2.7; **6063-T6 Al Selected**

Permissible Deviations for Ranges in Nominal Lengths (mm)	Tolerance Class Designation (Description)			
	f (fine)	m (medium)	c (coarse)	v (very coarse)
0.5 up to 3	±0.05	±0.1	±0.2	-
over 3 up to 6	±0.05	±0.1	±0.3	±0.5
over 6 up to 30	±0.1	±0.2	±0.5	±1.0
over 30 up to 120	±0.15	±0.3	±0.8	±1.5
over 120 up to 400	±0.2	±0.5	±1.2	±2.5
over 400 up to 1000	±0.3	±0.8	±2.0	±4.0
over 1000 up to 2000	±0.5	±1.2	±3.0	±6.0
over 2000 up to 4000	-	±2.0	±4.0	±8.0

Figure B.3 – ISO General Tolerance Tables

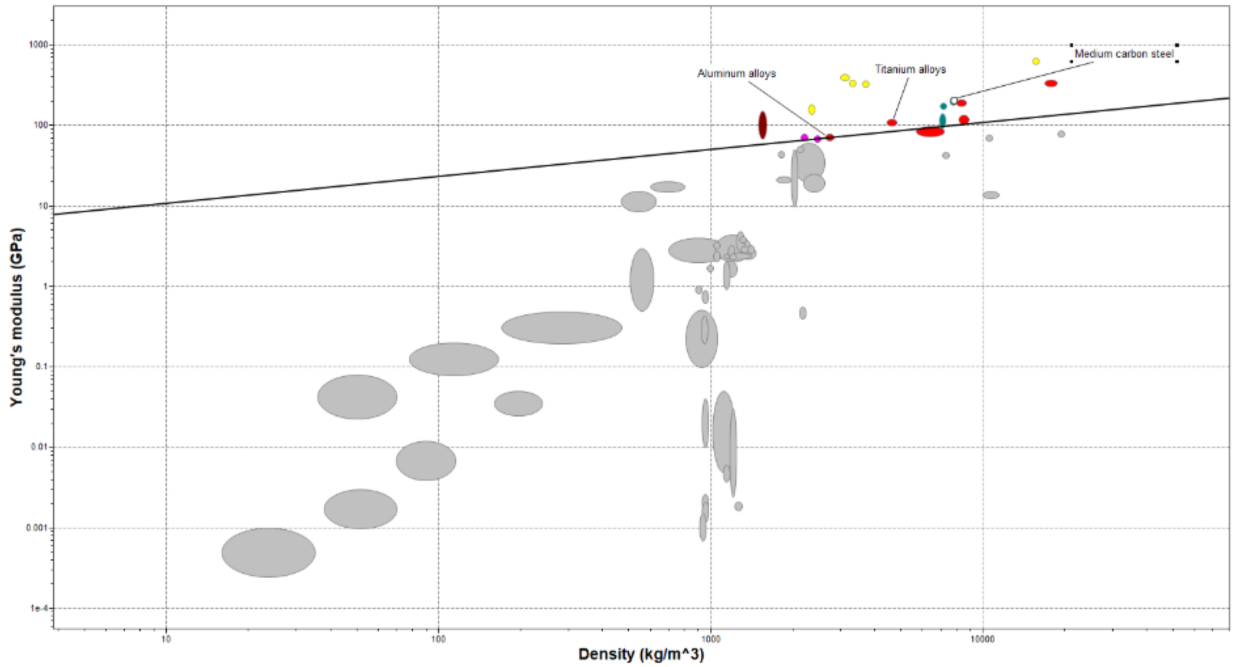

Figure B.4 Ashby chart of Young's Modulus for general materials

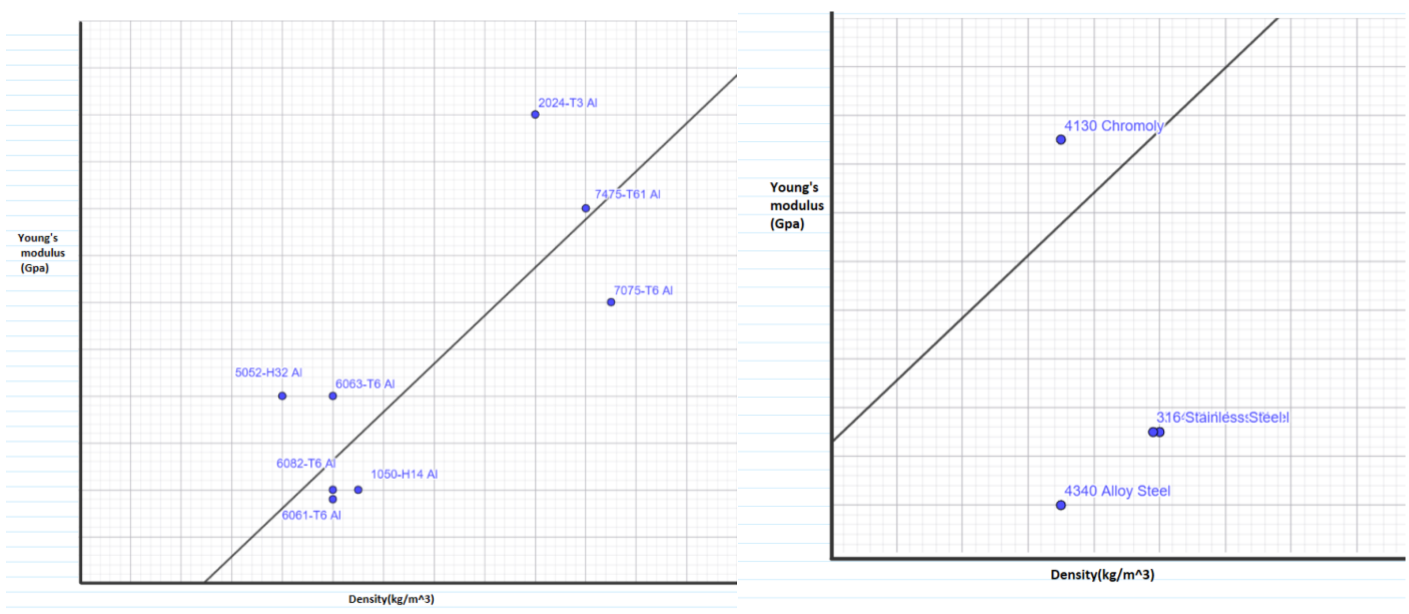

Figure B.5 - Ashby charts of Young's modulus verses density for candidate structural materials

Appendix C Z-Stage

C.1 Motion Profile

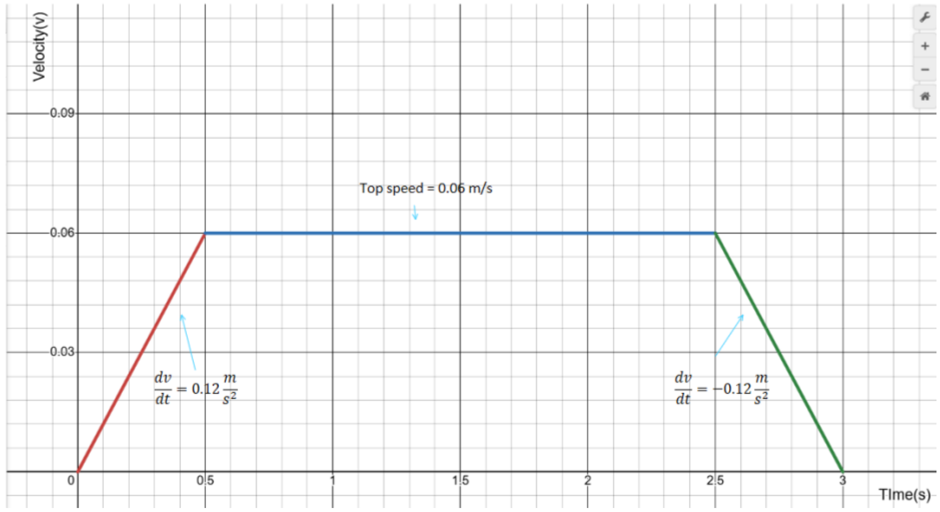

Figure C.1 - Velocity-time graph for the load-optimal motion profile along the Z-axis

The load-optimal motion profile ensures that the least acceleration takes place such that the inertial load induced by the acceleration is the least compared to all the other methods.

The velocity-time profile used for Z-stage assumes symmetric acceleration and deceleration phase, with a total travelled distance of 150mm completed within 3 seconds.

C.2 - Load Calculations for Linear Rails

The maximum applied radial load considering a safety factor of 4 comes out to be:

$$F_{Design} = 131.02 \times 4 = 524.08\ N$$

On each carriage this force will be half:

$$F_{Carriage} = \frac{524.08}{2} = 262.04\ N$$

The load of 262.04 N on each carriage is comfortably less than the rating of the selected linear rails. And it is also the smallest in the catalogue to meet the rail length requirement.

Model No.	Random-matching type	Assembly			Ball slide													Rail							Basic load rating (*2)							Ball diameter	Weight	
		Height			Width	Length	Mounting hole								Oil hole			Width	Height	Pitch	Mounting bolt hole		G	Maximum length	Dynamic	Static	Static moment (N·m)						Ball slide	Rail
																											M_{RO}	M_{PO}		M_{YO}				
		H	E	W_2	W	L	B	J	M×Pitch×ℓ	B_1	L_1	J_1	K	T	Hole diameter	T_1	N	W_1	H_1	F	d×D×h	B_3	(Reference)	L_{0max}	C (N)	C_0 (N)		one slide	two slides in close contact	one slide	two slides in close contact	D_w	(g)	(g/100 mm)
PU05TR	—	6	1	3.5	12	19.4	8	—	M2×0.4×1.5	2	11.4	5.7	5	2.3	ø0.9	1.5	—	5	3.2	15	2.3×3.3×0.8	2.5	5	210	520	775	2.06	1.28	9.90	1.28	9.90	1	4	11
PU07AR	—	8	1.5	5	17	23.4	12	8	M2×0.4×2.4	2.5	13.3	2.65	6.5	2.45	ø1.5	1.8	—	7	4.7	15	2.4×4.2×2.3	3.5	5	375	1 090	1 370	5.20	2.70	21.8	2.70	21.8	1.5875	8	23
PU09TR PU09UR	○	10	2.2	5.5	20	30 41	15	10 16	M3×0.5×3	2.5	19.6 30.6	4.8 7.3	7.8	2.6	—	—	—	9	5.5	20	3.5×6×4.5	4.5	7.5	600	1 490 2 100	2 150 3 500	9.90 16.2	6.10 15.6	41.0 88.0	6.10 15.6	41.0 88.0	1.5875	16 25	35
PU12TR PU12UR	○	13	3	7.5	27	35 48.7	20	15 20	M3×0.5×3.5	3.5	20.4 34.1	2.7 7.05	10	3.4	—	—	—	12	7.5	25	3.5×6×4.5	6	10	800	2 830 4 000	3 500 5 700	21.1 34.5	11.4 28.3	73.5 174	11.4 28.3	73.5 174	2.3812	32 53	65
PU15AL PU15BL	○	16	4	8.5	32	43 61	25	20 25	M3×0.5×5	3.5	26.2 44.2	3.1 9.6	12	4.4	ø3 (*1)	3.2	(3.6)	15	9.5	40	3.5×6×4.5	7.5	15	1 000	5 550 8 100	6 600 11 300	49.5 84.5	25.6 69.5	190 435	25.6 69.5	190 435	3.175	59 100	105

Table C.1 - Linear Rail dimension and load ratings (NSK Linear Guide Catalogue)

C.3 - Leadscrew Analysis

Buckling

Based on the total moving weight value of 248.7 N obtained from the upward acceleration, and applying a safety factor of 4, the maximum upper-bound approximation of the compressive force is 1100N. From Figure C.2 below, we can see that the curve for a leadscrew of diameter 8 has a slightly lower buckling load than we need, around 889N, hence with some interpolation, we can deduce that to satisfy the safety factor of 4, the leadscrew's minor diameter must be greater than 9. Since the distance between the two bearings are

450mm accounting for the full travel length and the moving length, we take the value from the 510mm vertical line.

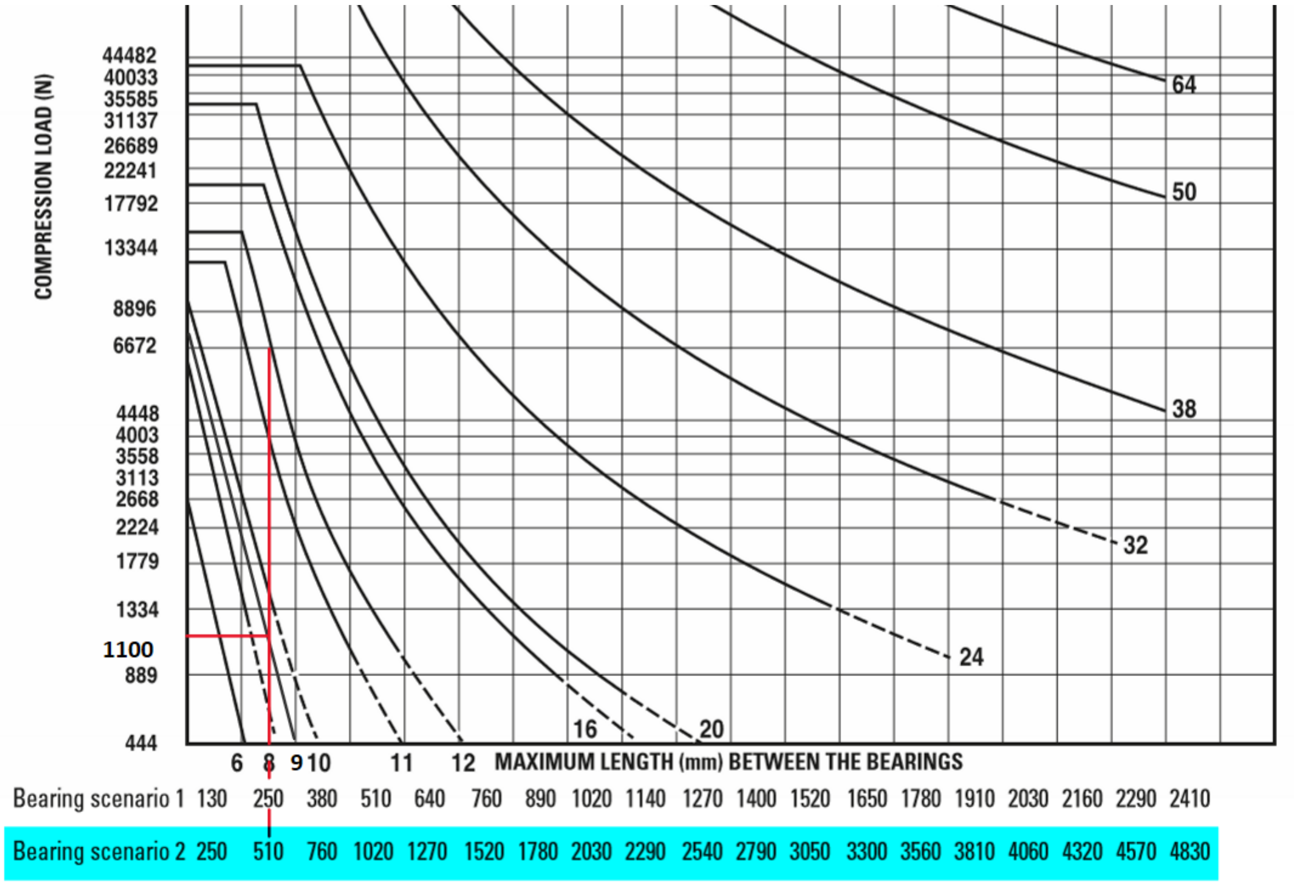

Figure C.2 - Showing the graph for maximum compressive load against maximum length for different diameters of leadscrews, and the bearing scenario in this project (Thomson BSA Catalogue)

Therefore, to fulfill these requirements obtained above, we looked at the leadscrew table in the Thomson BSA leadscrew catalogue (Table 3), and calculated the torque values for each leadscrew with a minor diameter greater than 8, using the below formula:

$$Torque = \frac{Load \times Lead}{2\pi\eta} = \frac{248.7 \times 0.004}{2 \times \pi \times 0.54} = 0.29\ Nm$$

Where is the efficiency η of the leadscrew given by the Thomson catalogue.

After evaluating the torque values for each of the leadscrews, the one with the lowest torque value was selected, as that would mean a smaller motor is needed, which can significantly help minimise costs during the motor selection stage. Hence the selected leadscrew was the SRA 2-12 x 2M leadscrew, with a lead of 4 and inner diameter 9.2.

12	3*	SPT	SRT	12 x 3M	8.0	48
	4	SPR	SRA	2-12 x 2M	9.2	54
	5^	SPT	SRT	2-12 x 2.5M	8.9	59
	6	SPR	SRA	3-12 x 2M	9.1	63
	10^	SPT	SRT	4-12 x 2.5M	8.9	73
	15	SPR	SRA	6-12 x 2.5M	8.7	78
	25	-	SRA	10-12 x 2.5M	9.2	82
	45	-	SRA	15-12 x 3M	9.6	81

Table C.2 - Showing the leadscrew dimensions and efficiency values (Thomson BSA Catalogue)

Shaft Whip and Angular Speed

Bearing scenario 2 was considered, in which the bearings are placed on the two ends of the lead screw:

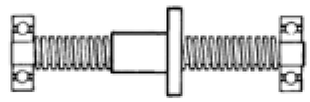

Bearing scenario 2

Figure C.3 – Showing the bearing arrangement

To check for shaft whip of the selected leadscrew, we used the values from Figure C.3, to obtain that the maximum angular speed of the shaft to be 1200 RPM.

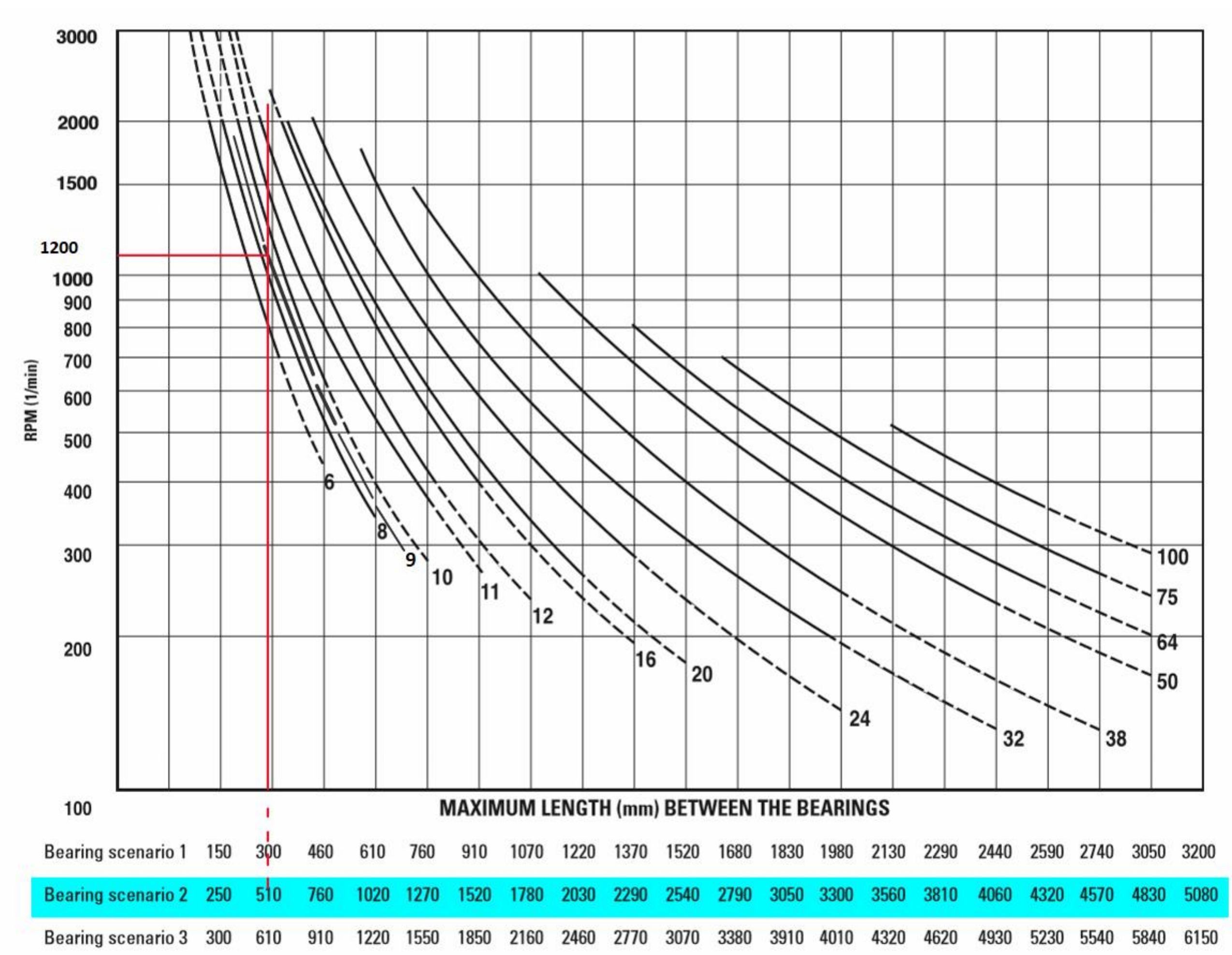

Figure C.4 - Graph showing the maximum RPM value against Maximum length for different diameters of leadscrews, as well as selected bearing scenario for this project (Thomson BSA Catalogue)

To calculate the max RPM of the lead screw, we considered that the maximum linear speed would be 0.06 m/s, as shown in figure C.1, and using the lead of 4mm, the rpm could be calculated as:

$$Angular\ Speed = \frac{Linear\ speed\left(\frac{m}{s}\right) \times 60}{Lead(m)} = \frac{0.06 \times 60}{0.004} = 900\ RPM$$

which is below the limit of 1200 RPM from Figure C.3.

We also calculate the required mechanical power for the lead screw:

$$Power(W) = Torque(Nm) \times \frac{2\pi \times RPM}{60} = \frac{0.29 \times 2 \times \pi \times 900}{60} = 27.3\ W$$

The mechanical power requirement is 27.3 W.

C.4 – Bearing Selection

Bearing Number	Nominal Bearing Dimensions						Preferred Shoulder Diameters						Basic Load Ratings				Limiting Speeds (RPM)		Bearing Weight (Approx.)	
	d		D		B		r*		Shaft		Housing		C_r		C_{or}					
	mm	inch	mm	inch	mm	inch	mm	inch	mm	inch	mm	inch	N	lbs	N	lbs	Grease	Oil	g	lbs
689	9	0.3543	17	0.6693	4.0	0.1575	0.20	0.007	10.6	0.417	15.4	0.606	1330	299	665	149	36000	43000	3.53	0.007
689ZZ\VV	9	0.3543	17	0.6693	5.0	0.1969	0.20	0.007	11.5	0.453	15.2	0.598	1330	299	665	149	36000	43000	4.43	0.009
609	9	0.3543	24	0.9449	7.0	0.2756	0.30	0.011	11.0	0.433	22.8	0.898	3350	755	1430	320	32000	38000	14.50	0.029
629	9	0.3543	26	1.0236	8.0	0.3150	0.30	0.011	11.0	0.433	24.0	0.945	4550	1030	1970	445	28000	34000	19.50	0.044

Table C.3 - Showing the 600-series bearing dimensions and load ratings (NSK Ball Bearings Catalogue)

Life Calculation

The formula for calculating bearing life in hours:

$$L_{10} = \frac{\left(\frac{C_r}{F_{axial}}\right)^a \times 10^6}{60 \times n}$$

The constant 'a' is 3 for ball bearings.

$$L_{10} = \frac{\left(\frac{1430}{248.7}\right)^3 \times 10^6}{60 \times 900}$$

$$L_{10} = 3520\ Hours$$

C.5 – Stage Deflection

The total deflection at the top of the edge due to the applied couple is calculated using:

$$y = \frac{1}{6}\left(\frac{4F_1L^3}{ECt^3} - \frac{4F_2a^3}{ECt^3}\left(1 + \frac{3b}{2a}\right)\right)$$

$$y = \frac{1}{6}\left(\frac{4 \times 131.02 \times 0.45^3}{(68.9 \times 10^9) \times 0.165 \times 0.0542^3} - \frac{4 \times 131.02 \times 0.15^3}{(68.9 \times 10^9) \times 0.165 \times 0.0542^3}\left(1 + \frac{3 \times 0.3}{2 \times 0.15}\right)\right) = 3.746\ \mu m$$

C.6 – Motor and Gearbox

Plotting the operating point on the motor performance diagram shows that it lies in the continuous-operation region with reduced thermal resistance.

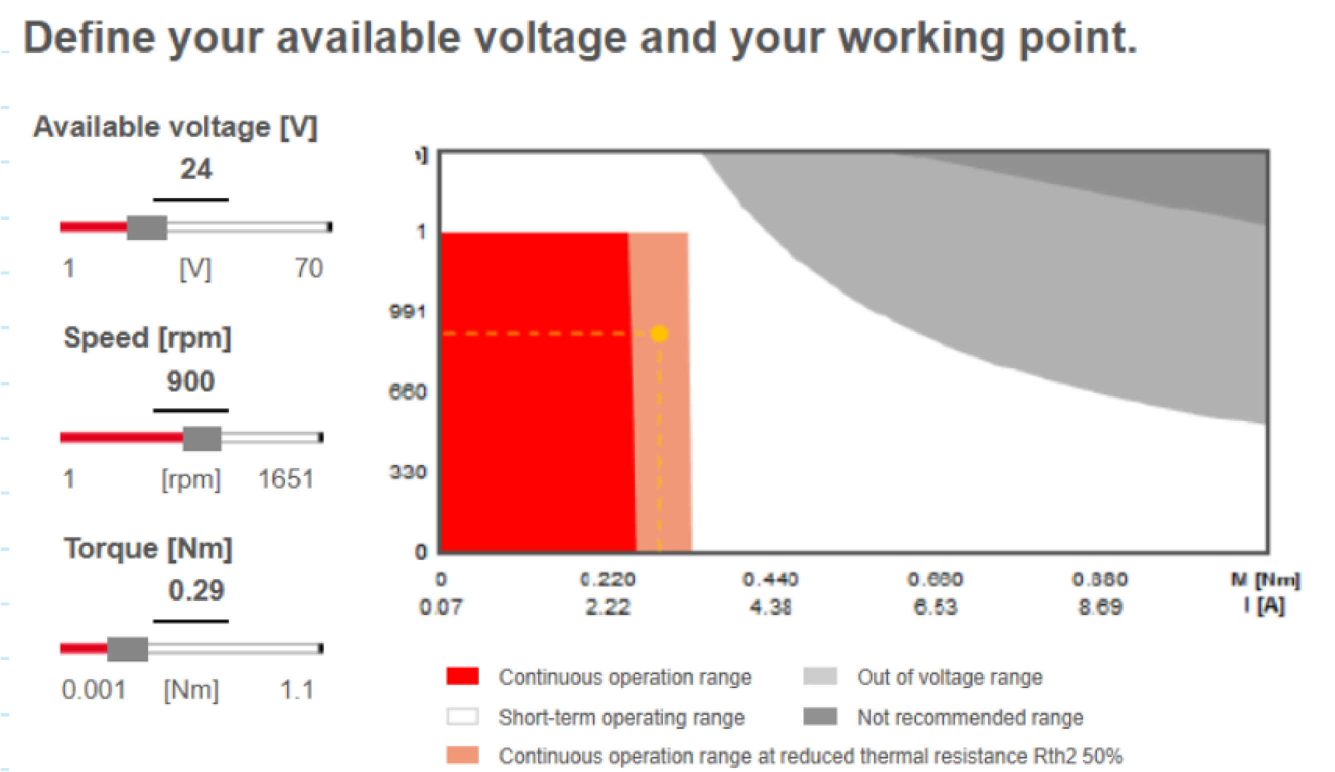

Figure C.5 - Speed-Torque plot of the Motor & Gearbox (Maxon Configurator)

Appendix D – Y-Stage

D.1 – Motion Profile

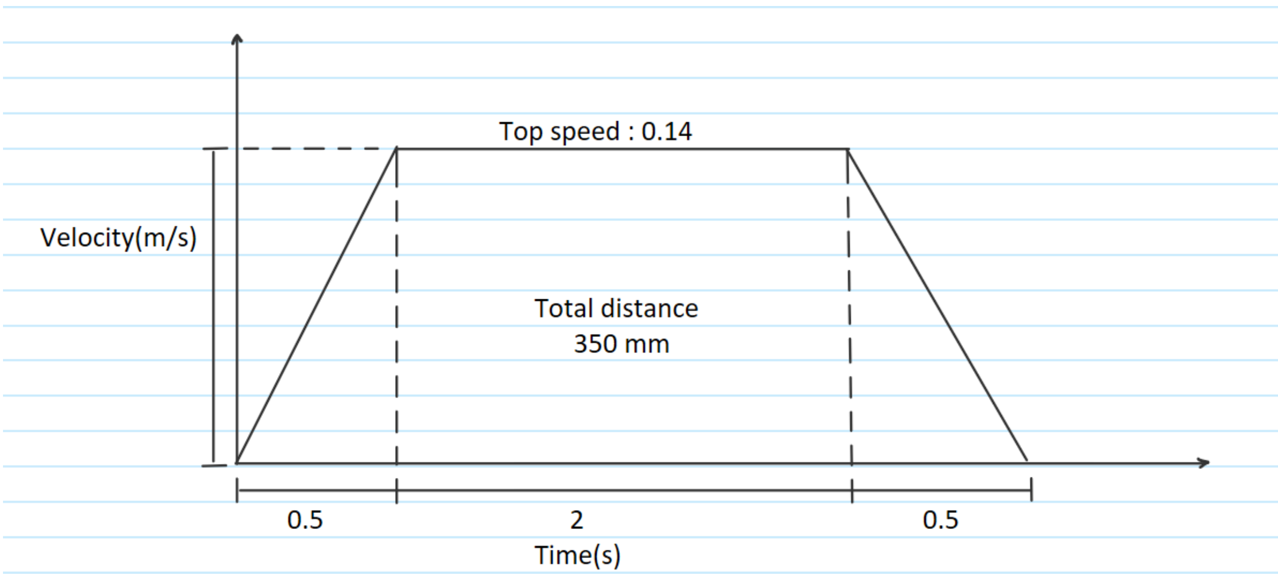

Figure D.1 - Velocity-time graph for the load-optimal motion profile along the Y-axis

Acceleration:

$$a = \frac{v}{t} = \frac{0.14}{0.5} = 0.28\, ms^{-2}$$

Max linear velocity:

$$v = 0.14\, ms^{-2}$$

Despite the larger mass compared to the Z stage, the force required is lower because the Y stage does not act against gravity.

D.2 – Load Determination

The Y stage consists of the Z stage mounted on top, along with additional components that allow motion in the horizontal (Y) direction. The main loads acting on the Y stage come from the Z stage. These loads can be broken down into one vertical load and two moments and all these loads are supported by the linear rails.

Step 1: Moment caused by force F_1:

$$M_1 = F_1 \times l$$

$$M_1 = 131.02 \times 0.52 = 68.13$$

This moment is then converted into forces acting on the rails:

$$F_3' = \frac{M_1}{2a}$$

$$F'_1 = \frac{68.13}{2 \times 0.15} = 227.10$$

$$F_4' = -F_3'$$

Step 2: Moment caused by force F_2:

$$M_2 = F_2 \times c$$

$$M_1 = 131.02 \times 0.49$$

The resulting forces on the rails are:

$$F_3'' = \frac{M_2}{2a}$$

$$F''_3 = \frac{64.2}{2 \times 0.15} = 214.00$$

$$F_4'' = -F_3''$$

Step 3: Forces due to the weight of the vertical stage:

$$F_3''' = F_4''' = \frac{\text{Load}}{2}$$

$$F'''_3 = F'''_4 = \frac{665.5}{2} = 332.75$$

Step 4: Combined forces on each rail:

$$F_3 = F_3' + F_3'' + F_3'''$$
$$F_4 = F_4' + F_4'' + F_4'''$$

$$F_3 = F_4 = 773.86$$

Forces on individual carriages

$$F_{3a} = F_{3b} = \frac{F_3}{2}$$

$$F_{3a} = F_{3b} = \frac{773.86}{2} = 386.93$$

We get a force of 386.93 N on each recirculating bearing

To ensure safe operation, a safety factor of 4 is applied:

$$386.93 \times 4 = 1547.72\, N$$

The minimum rail length can be calculated as:

$$L_{min} = Minimum\ required\ Yaxis\ travel + Length\ of\ Yaxis\ base\ plate$$

$$L_{min} = 350 + 255 = 605\, mm$$

Model No.	Random-matching type	Assembly Height			Ball slide Width	Length	Mounting hole								Oil hole			Rail Width	Height	Pitch	Mounting bolt hole		G	Maximum length	Dynamic	Static
		H	E	W_2	W	L	B	J	M×Pitch×ℓ	B_1	L_1	J_1	K	T	Hole diameter	T_1	N	W_1	H_1	F	d×D×h	B_3	(Reference)	L_{0max}	C (N)	C_0 (N)
PU05TR	—	6	1	3.5	12	19.4	8	—	M2×0.4×1.5	2	11.4	5.7	5	2.3	ø0.9	1.5	—	5	3.2	15	2.3×3.3×0.8	2.5	5	210	520	775
PU07AR	—	8	1.5	5	17	23.4	12	8	M2×0.4×2.4	2.5	13.3	2.65	6.5	2.45	ø1.5	1.8	—	7	4.7	15	2.4×4.2×2.3	3.5	5	375	1 090	1 370
PU09TR PU09UR	○	10	2.2	5.5	20	30 41	15	10 16	M3×0.5×3	2.5	19.6 30.6	4.8 7.3	7.8	2.6	—	—	—	9	5.5	20	3.5×6×4.5	4.5	7.5	600	1 490 2 100	2 150 3 500
PU12TR PU12UR	○	13	3	7.5	27	35 48.7	20	15 20	M3×0.5×3.5	3.5	20.4 34.1	2.7 7.05	10	3.4	—	—	—	12	7.5	25	3.5×6×4.5	6	10	800	2 830 4 000	3 500 5 700
PU15AL PU15BL	○	16	4	8.5	32	43 61	25	20 25	M3×0.5×5	3.5	26.2 44.2	3.1 9.6	12	4.4	ø3 (*1)	3.2	(3.6)	15	9.5	40	3.5×6×4.5	7.5	15	1 000	5 550 8 100	6 600 11 300

Table D.1 - Linear Rail dimension and load ratings (NSK Linear Guide Catalogue)

D.3 Leadscrew Analysis

Force Calculations

The force required to drive the Y stage is calculated using Newton's second law:

$$F = ma$$

Since the motion is horizontal, gravity does not act in the direction of motion, so $a = 0.28\ \frac{m}{s^2}$

Total moving mass is $67.84\ kg$

Thus,

$$F = 67.84 \cdot 0.28 = 19.00$$

Calculations for Torque and Angular Velocity:

$$T = \frac{F \times Lead}{2\pi\eta}$$

$$T = \frac{(19 \cdot 16)}{2\pi \cdot 0.75} = 64.51\ Nm$$

$$\omega_{RPM} = \frac{v \times 60}{Lead} = \frac{0.14 \times 60}{16 \times 10^{-3}} = 525\ RPM$$

Buckling and Shaft whip

Bearing scenario 2 was considered, in which the bearings are placed on the two ends of the lead screw:

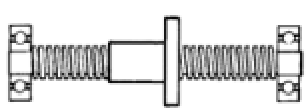

Bearing scenario 2

Figure D.2 – Showing the bearing arrangement

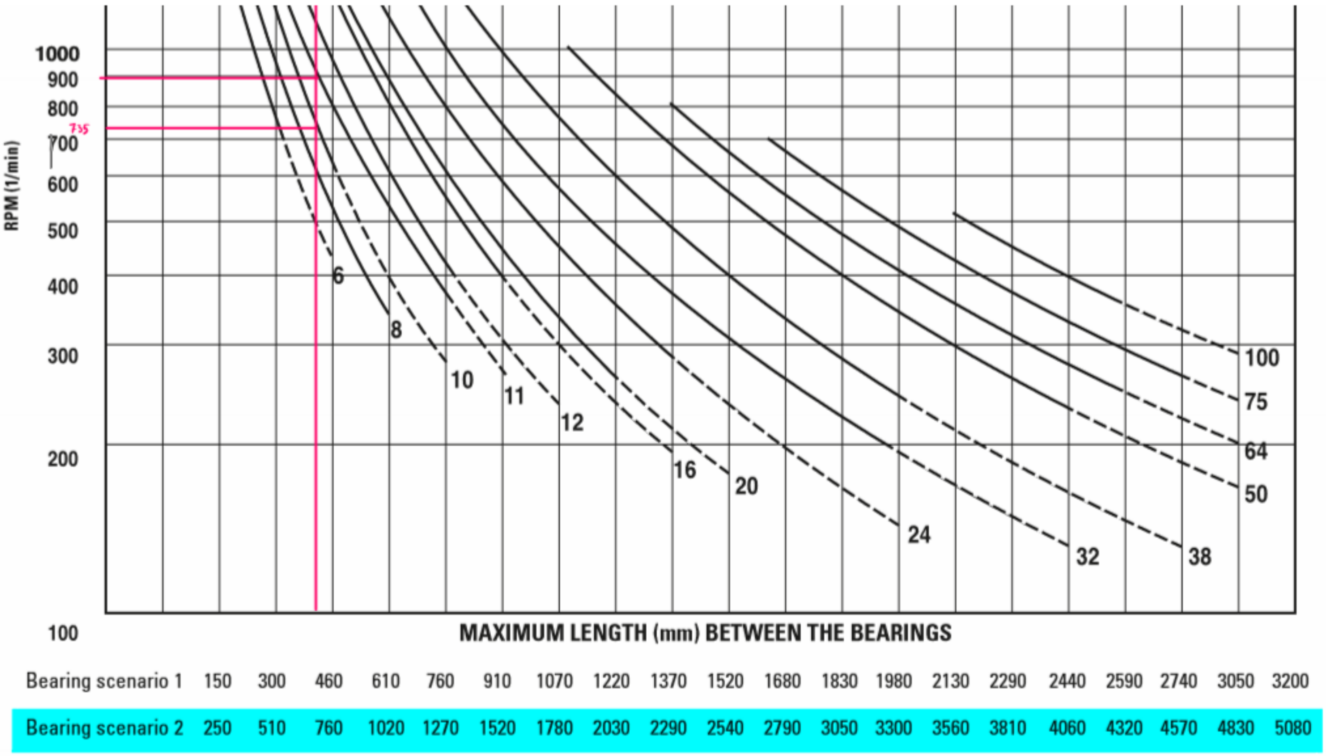

Figure D.3 - Showing the graph for angular speed against maximum length between bearings for different diameters of leadscrews (Thomson BSA Catalogue)

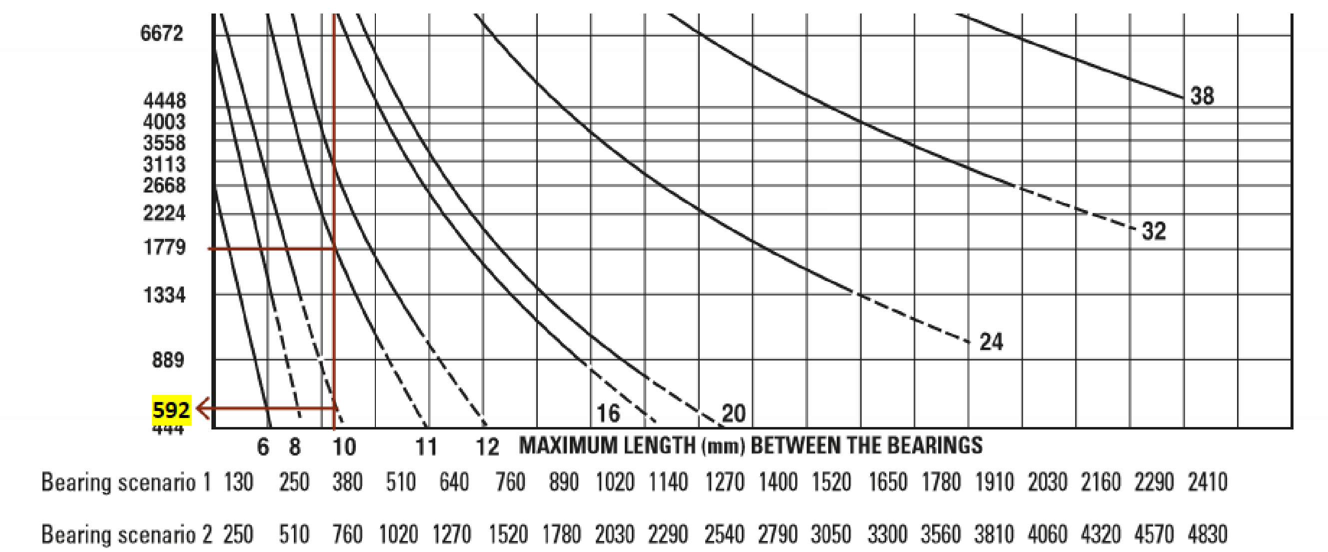

Figure D.4 - Showing the graph for maximum compressive load against maximum length between bearings for different diameters of leadscrews (Thomson BSA Catalogue)

16	4*	SPT	SRT	16 x 4M	11.3	48
	5	SPR	SRA	2-16 x 2.5M	12.2	52
	8	SPR	SRA	4-16 x 2M	13.0	63
	16	SPR	SRA	7-16 x 2.3M	12.6	75
	25	-	SRA	5-16 x 5M	11.5	80
	35	-	SRA	7-16 x 5M	12.2	82
20	4*	SPT	SRT	20 x 4M	15.3	42
	8	SPR	SRA	2-20 x 4M	14.8	59
	12	SPR	SRA	3-20 x 4M	15.0	67
	16	SPR	SRA	4-20 x 4M	15.0	72
	20	-	SRA	5-20 x 4M	15.0	76

Table D.2 showing leadscrew dimensions and efficiency values (Thomson BSA Catalogue)

D.4 Bearing Selection

Bearing Number	Basic Load Ratings				Factor	Limiting Speeds (RPM)		Bearing Weight (Approx.)	
	C_r		C_{or}						
	N	lbs	N	lbs	f_0	Grease	Oil	kg	lbs
6300	8500	1910	3450	770	11.2	26000	30000	0.052	0.12
6301	10200	2290	4200	940	11.1	24000	28000	0.060	0.13
6302	12000	2700	5450	1220	12.3	20000	24000	0.083	0.18
6303	14300	3200	6650	1490	12.4	18000	20000	0.113	0.25
6304	16700	3750	7900	1770	12.4	16000	19000	0.145	0.32
6305	21600	4850	11200	2530	13.2	13000	16000	0.235	0.52
6306	28000	6300	15000	3400	13.3	11000	13000	0.345	0.76

Table D.3 – Showing 6300 series bearing load ratings

Bearing Number	Nominal Bearing Dimensions						Preferred Shoulder Diameters							
	d		D		B		r**		da/db				Da	
									min		max		max	
	mm	inch	mm	inch	mm	inch	mm	inch	mm	inch	mm	inch	mm	inch
6300	10	0.3937	35	1.3780	11	0.4331	0.6	0.023	14.0	0.551	16.5	0.650	31.0	1.220

Table D.4 – Showing dimensions for the 6300 bearing.

Calculation for bearing fatigue life:

$$L_{10,Hours} = \frac{\left(\frac{C_{0r}}{F_{eq}}\right)^{a} \times 10^{6}}{60 \times n}$$

$$L_{10,Hours} = \frac{\left(\frac{3450}{665.5}\right)^{3} \times 10^{6}}{60 \times 525}$$

$$L_{10,Hours} = 4423\ Hours$$

D.5 Motor and Gearbox

	Leadscrew	GB (6.6)	GB efficiency <- Motor

Torque (Nmm)	64.51	9.77	10.86
Angular speed(rpm)	525	3465	3465

Table D.5 – Showing required motor torque and angular speed

DCX 19 S Ø19 mm, precious metal brushes, ball bearings	19 mm	5 W	24 V	6350 rpm	11 mNm	**€169.15**
DCX 19 S Ø19 mm, graphite brushes, ball bearings	19 mm	11 W	12 V	12700 rpm	11.4 mNm	**€166.10**
DCX 19 S Ø19 mm, graphite brushes, ball bearings	19 mm	11 W	24 V	12700 rpm	11.4 mNm	**€166.10**
DCX 19 S Ø19 mm, graphite brushes, ball bearings	19 mm	11 W	48 V	12700 rpm	11.5 mNm	**€166.10**

Figure D.5 – showing similar motors and their specifications and cost

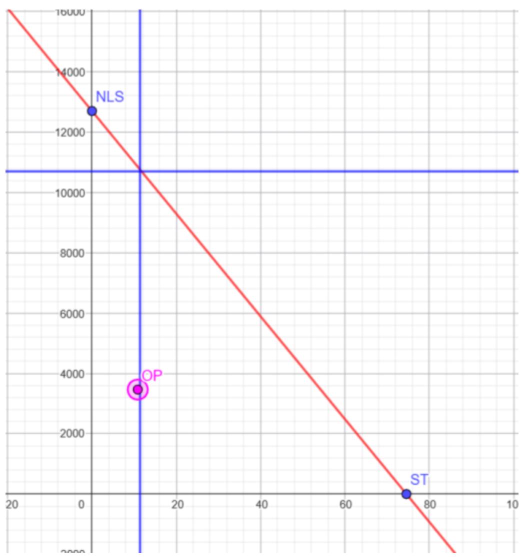

Figure D.6 – Speed-Torque diagram of the motor

Operating conditions under motor graph and in behind nominal area so it the best operating condition.

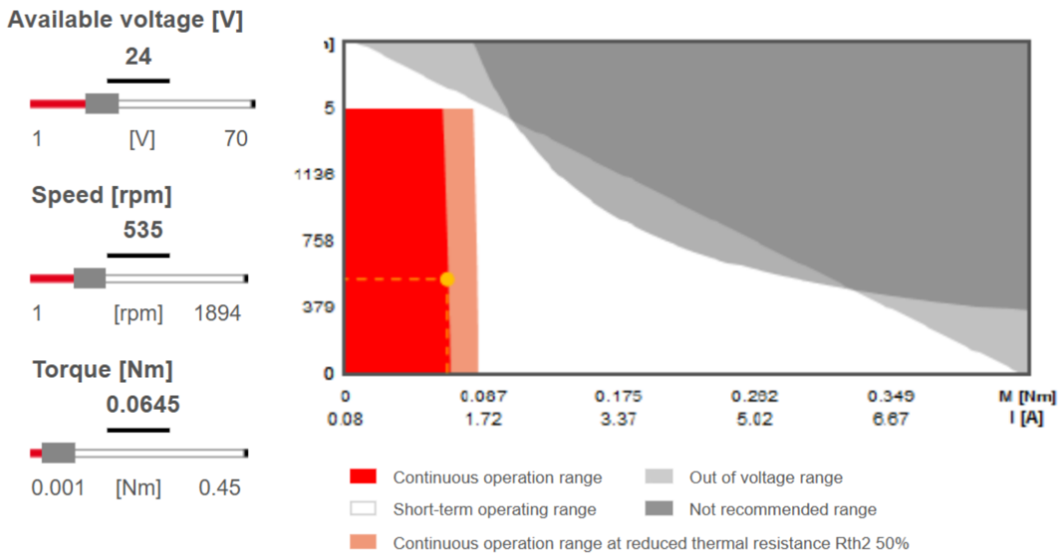

Figure D.7 - Speed-Torque plot of the Motor & Gearbox (Maxon Configurator)

D.6 Deflection of Y axis stage

The sources of deflection for the Y plate can be due to its own weight as well as the two applied forces from the Z stage

Considering half of the Y axis

Deflection from all three forces was calculated and summed.

1) Deflection due to uniformly distributed load

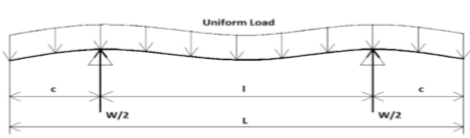

$$y_{\text{uniform}} = \frac{W(l+c)}{24EIL}[3c^2(c+2l) - l^3]$$

$$y_{uniform} = \frac{91.54(0.34+0.15)}{24 \times (6.89 \times 10^{10}) \times (4.05 \times 10^{-7}) \times 0.64} \times [3 \times 0.15^2(0.15 + 2 \times 0.34) - 0.34^3]$$

2) Deflection due to force F_3

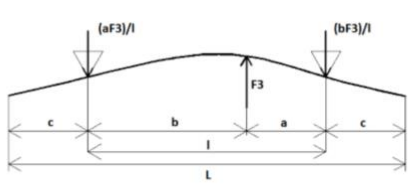

$$y_{F_3} = \frac{F_3\, abc}{6EI}(l+b)$$

$$y_{F_3} = \frac{386.93 \times 0.19 \times 0.25 \times 0.1}{6 \times (6.89 \times 10^{10}) \times (4.05 \times 10^{-7})} \times (0.44 + 0.25)$$

3) Deflection due to force F_4

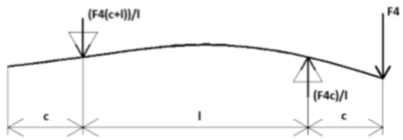

$$y_{F_4} = \frac{F_4\, c^2}{6EI}(c + l)$$

$$y_{F_4} = \frac{386.93 \times 0.15^2}{6 \times (6.89 \times 10^{10}) \times (4.05 \times 10^{-7})} \times (0.15 + 0.34)$$

4) Total (integrated) deflection

$$y = y_{\text{uniform}} + y_{F_3} + y_{F_4}$$

$$y = (0.89 + 2.38 + 1.72) = 4.9\,\mu m$$

E = Young's modulus
I = second moment of area
W = total uniformly distributed load
F_3, F_4= applied point forces
a, b, c, l, L= geometric distances shown in the diagrams
of 4.9 µm, satisfying the stiffness requirement.

Appendix E – X-Stage

E. 1 – Motion Profile

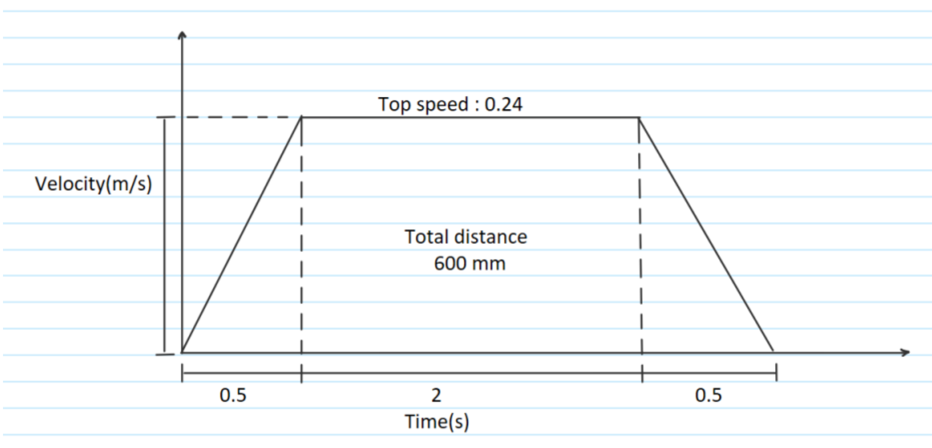

Figure E.1 – velocity-time graph for load optimal motion

Finding the acceleration of the stage geometrically:

$$600 = 2v(0.5)^2 + 2v \rightarrow \; v = 0.24$$

$$a = \frac{dv}{dt} = \frac{0.25}{0.5} = 0.48ms^{-2}$$

E.2 – Load Determination

The calculations were automated on Excel for different bearing spacings.

Contributions to F_5 and F_6 from F_3:

$$M_1 = 636.9 * 0.07 = 44.58$$

$$F_{5,1} = \frac{44.58}{0.3} = 148.6$$

$$F_{6,1} = 636.9 - 148.6 = 488.3$$

Contributions to F_5 and F_6 from F_4:

$$M_2 = 636.9 * 0.07 = 108.3$$

$$F_{5,2} = \frac{108.3}{0.3} = 361$$

$$F_{6,2} = 636.9 + 361 = 997.9$$

Contributions to F_5 and F_6 from the weight:

$$F_{5,3} = F_{6,3} = \frac{436.9}{2} = 218.5$$

Sum of each contribution:

$$F_5 = 728.0N \; and \; F_6 = 1704.6N$$

Loads on individual bearings:

$$F_{5'} = 364.0N \; and \; F_{6'} = 852.3N$$

Table 13 Dimensions (PU series)

Model No.	Random-matching type	Assembly Height H	Assembly E	Assembly W_2	Ball slide Width W	Ball slide Length L	Mounting hole B	Mounting hole J	Mounting hole MxPitchxℓ	B_1	L_1	J_1	K	T
PU05TR	—	6	1	3.5	12	19.4	8	—	M2x0.4x1.5	2	11.4	5.7	5	2.3
PU07AR	—	8	1.5	5	17	23.4	12	8	M2x0.4x2.4	2.5	13.3	2.65	6.5	2.45
PU09TR	○	10	2.2	5.5	20	30	15	10	M3x0.5x3	2.5	19.6	4.8	7.8	2.6
PU09UR						41		16			30.6	7.3		
PU12TR	○	13	3	7.5	27	35	20	15	M3x0.5x3.5	3.5	20.4	2.7	10	3.4
PU12UR						48.7		20			34.1	7.05		
PU15AL	○	16	4	8.5	32	43	25	20	M3x0.5x5	3.5	26.2	3.1	12	4.4
PU15BL						61		25			44.2	9.6		

Model No.	Oil hole Hole diameter	Oil hole T_1	Oil hole N	Rail Width W_1	Rail Height H_1	Rail Pitch F	Mounting bolt hole dxDxh	B_3	G (Reference)	Maximum length L_{0max}	Basic loa[d] Dynamic C (N)	Static C_0 (N)	M_{RO} one slide
PU05TR	ø0.9	1.5	—	5	3.2	15	2.3x3.3x0.8	2.5	5	210	520	775	2.06	1.28
PU07AR	ø1.5	1.8	—	7	4.7	15	2.4x4.2x2.3	3.5	5	375	1 090	1 370	5.20	2.70
PU09TR	—	—	—	9	5.5	20	3.5x6x4.5	4.5	7.5	600	1 490	2 150	9.90	6.10
PU09UR											2 100	3 500	16.2	15.6
PU12TR	—	—	—	12	7.5	25	3.5x6x4.5	6	10	800	2 830	3 500	21.1	11.4
PU12UR											4 000	5 700	34.5	28.3
PU15AL	ø3 (*1)	3.2	(3.6)	15	9.5	40	3.5x6x4.5	7.5	15	1 000	5 550	6 600	49.5	25.6
PU15BL											8 100	11 300	84.5	69.5

Table E.1 - Linear Rail dimension and load ratings (NSK Linear Guide Catalogue)

$$Max \; load \; on \; bearing * SF = 852.3 * 4 = 3409.2$$

$$3409.2 < 4000$$

The selected linear bearing and rail combination is the smallest rated to both take the required loads and travel the distance necessary for the X stage of 640mm.

E.3- Leadscrew Analysis

The leadscrew was selected iteratively through Excel, substituting values from the catalog into equations and verifying that they were reasonable for motor calculations, while checking that there were bearings available for the minor diameter specified that could take the required loads. The smallest leadscrew to meet these requirements is the 5-20x4M leadscrew.

16	8	SPR	SRA	4-16 x 2M	13.0	63
	16	SPR	SRA	7-16 x 2.3M	12.6	75
	25	-	SRA	5-16 x 5M	11.5	80
	35	-	SRA	7-16 x 5M	12.2	82
20	4*	SPT	SRT	20 x 4M	15.3	42
	8	SPR	SRA	2-20 x 4M	14.8	59
	12	SPR	SRA	3-20 x 4M	15.0	67
	16	SPR	SRA	4-20 x 4M	15.0	72
	20	-	SRA	5-20 x 4M	15.0	76
	45	-	SRA	9-20 x 5M	15.8	82
	50	-	SRA	10-20 x 5M	16.5	82
24	5*	SPT	SRT	24 x 5M	18.5	42

Table E.2 showing leadscrew dimensions and efficiency values (Thomson BSA Catalogue)

Finding force, torque and angular velocities:

$$F = 112.3 \cdot 0.48 = 53.90$$

$$T = \frac{(53.9 \cdot 20)}{2\pi \cdot 0.76} = 225.77Nmm$$

$$v = 0.24m/s$$

$$\omega = \frac{240}{20} \cdot 60 = 720rpm$$

Operating speed: 720rpm

Bearing arrangement: Scenario 2

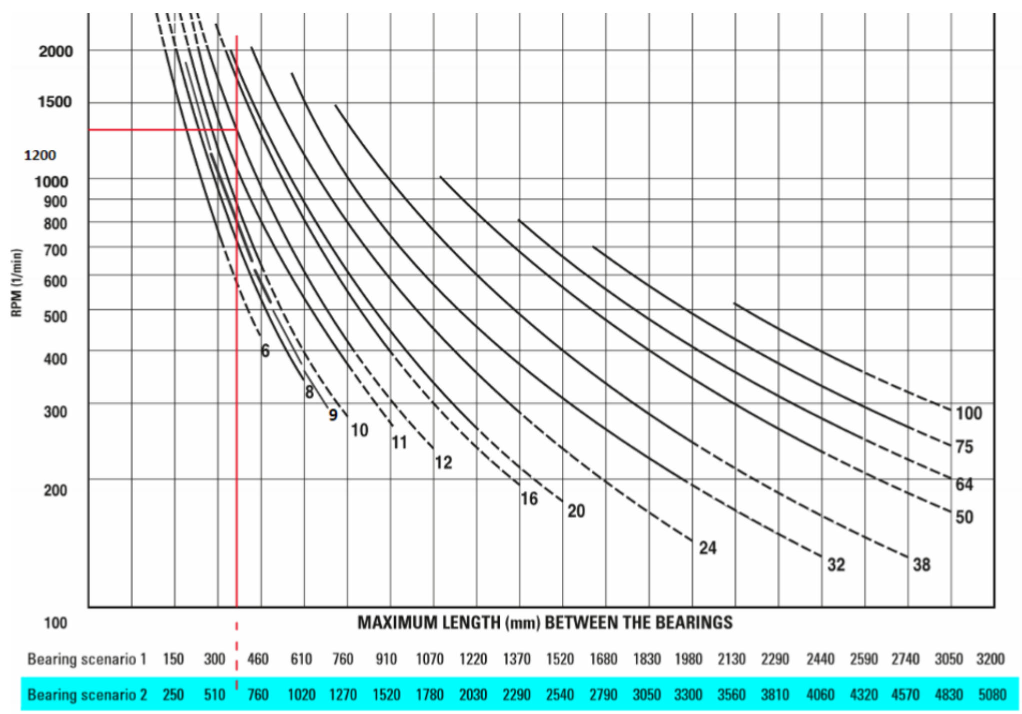

Figure E.2 - Showing the graph for maximum compressive load against maximum length for different diameters of leadscrews, and the bearing scenario in this project (Thomson BSA Catalogue)

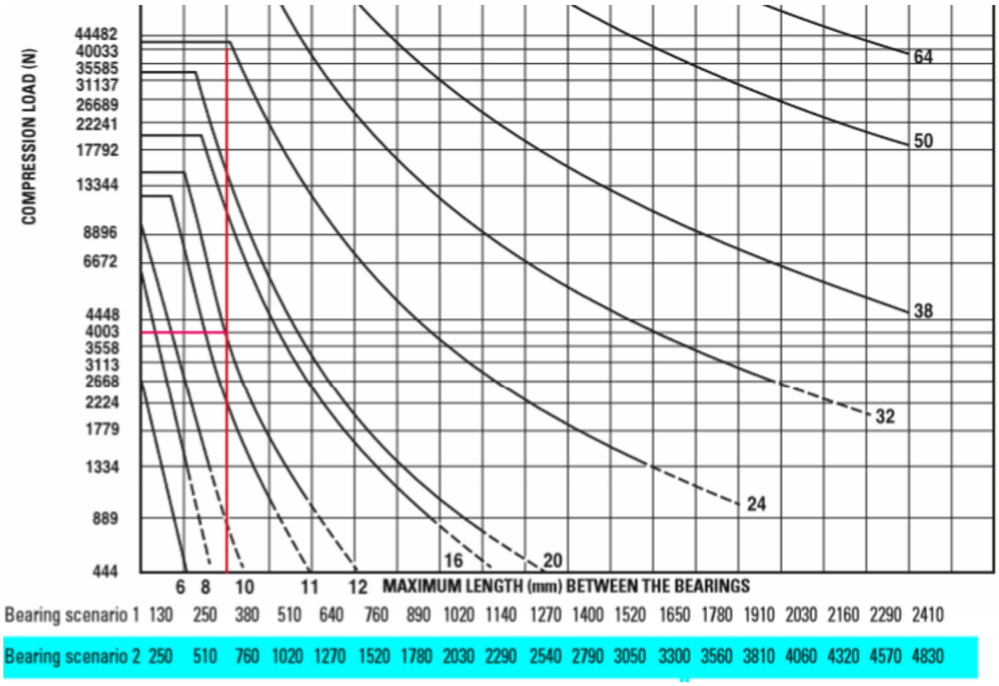

Figure E.3 - Showing the graph for maximum compressive load against maximum length for different diameters of leadscrews, and the bearing scenario in this project (Thomson BSA Catalogue)

The graphs show the maximum compressive load and rpm for the 2-bearing mounting chosen for the leadscrew at a length of 640mm. The minor diameter of our leadscrew is 15mm, so we have followed the 12mm diameter line on the graphs rather than the 16mm one as an additional factor of safety. This gives us a maximum rotational speed of around 1300rpm and maximum compressive load of around 4000N, which amply cover 7200rpm and 215.6N (59.9N*4) calculated.

Model no.	Shaft diameter (mm)	May also be used with inch thread	Dimensions				Permissible dynamic load (N)	Drag torque	
			A (mm)	B (mm) max	C (mm)	TH (mm)		min. (Nmm)	max. (Nmm)
XCB3700	10	5/16, 3/8	20.8	47.6	6.4	M16 x 1.5	100	7	21
XCB5000	12	7/16, 1/2	28.4	57.2	9.5	M25 x 1.5	550	7	21
XCB6200	16	5/8	35.6	66.0	12.7	M30 x 1.5	775	14	42
XCB7500	20	3/4	41.4	73.7	12.7	M35 x 1.5	1100	21	71
XCB10000	24	1	47.8	76.2	15.2	M40 x 1.5	1550	35	71

Table E.3 - Lead screw nuts

E.4- Leadscrew Iteration

iterating	lead	efficiency	Torque (Nmm)	ang speed (rpm)	shaft d (mm)	max rpm (approx)	y/n	why?
3-12x2m	6	0.63	81.54796	2400	9.1	700	no	rpm high, bearings
15-12x3m	45	0.81	475.6964	320	9.6	700	no	T high, bearings
10-12x2.5m	25	0.82	261.0529	576	9.2	700	no	rpm high, bearings
5-16x5m	25	0.8	267.5792	576	11.5	900	no	bearings
7-16x5M	35	0.82	365.4741	411.4	12.2	1300	no	T high, bearings
5-20x4M	20	0.76	225.7487	720	15	1500	yes	good all around

Table E.4 Excel sheet showing leadscrew iterations

The Excel iterations initially failed to account that bearings had to have a small enough minor diameter to be press fit onto the leadscrew, causing the initial consideration of some inappropriate options. After correcting for this, the chosen screw was deemed to be appropriate, using the screening constraints of torques below 300mNm and rpm below 80% of max rpm.

E.5 Bearing Selection

Load calculation:

$$\frac{Fa}{Fr} = \frac{53.90}{1102} = 0.049$$

$$0.049 < 0.5$$

$$Feq = 1Fr \cdot 0Fa$$

$$Feq = 1102 \cdot 4 = 4408N$$

Bearing life calculation:

$$L_{10} = \frac{\left(\frac{C_{0r}}{F_{axial}}\right)^{a} \times 10^6}{60 \times n}$$

$$L_{10} = \frac{\left(\frac{5450}{1102}\right)^{3} \times 10^6}{60 \times 720}$$

$$L_{10} = 2800 Hours$$

Bearing has a suitable life span.

Bearing Number	Basic Load Ratings				Factor	Limiting Speeds (RPM)		Bearing Weight (Approx.)	
	C_r		C_{or}						
	N	lbs	N	lbs	f_0	Grease	Oil	kg	lbs
6300	8500	1910	3450	770	11.2	26000	30000	0.052	0.12
6301	10200	2290	4200	940	11.1	24000	28000	0.060	0.13
6302	12000	2700	5450	1220	12.3	20000	24000	0.083	0.18
6303	14300	3200	6650	1490	12.4	18000	20000	0.113	0.25
6304	16700	3750	7900	1770	12.4	16000	19000	0.145	0.32
6305	21600	4850	11200	2530	13.2	13000	16000	0.235	0.52
6306	28000	6300	15000	3400	13.3	11000	13000	0.345	0.76
6307*	35000	7850	19200	4300	13.2	10000	12000	0.464	1.01
6308*	43000	9600	24000	5400	13.2	9000	11000	0.636	1.40

Table E.5 – Showing 6300 series bearing load ratings

E.6 Motor and Gearbox

DCX 26 L Ø 26mm, CLL precious metal brushes, ball bearings	26 mm	22 W	24 V	5330 rpm	52.3 mNm	€271.04
DCX 26 L Ø 26mm, CLL precious metal brushes, ball bearings	26 mm	22 W	48 V	5320 rpm	50.3 mNm	€271.04
DCX 26 L Ø 26mm, graphite brushes, ball bearings	26 mm	40 W	12 V	10600 rpm	46.9 mNm	€267.99
DCX 26 L Ø 26mm, graphite brushes, ball bearings	26 mm	40 W	24 V	10700 rpm	57.8 mNm	€267.99
DCX 26 L Ø 26mm, graphite brushes, ball bearings	26 mm	40 W	48 V	10700 rpm	59.7 mNm	€267.99

Figure E.5 – showing similar motors and their specifications and cost

	Leadscrew	GB (5.3)	GB efficiency -> Motor
Torque (Nmm)	225.77	42.59	47.33
Angular speed(rpm)	720	3816	3816

Table E.6 – Showing required motor torque and angular speed

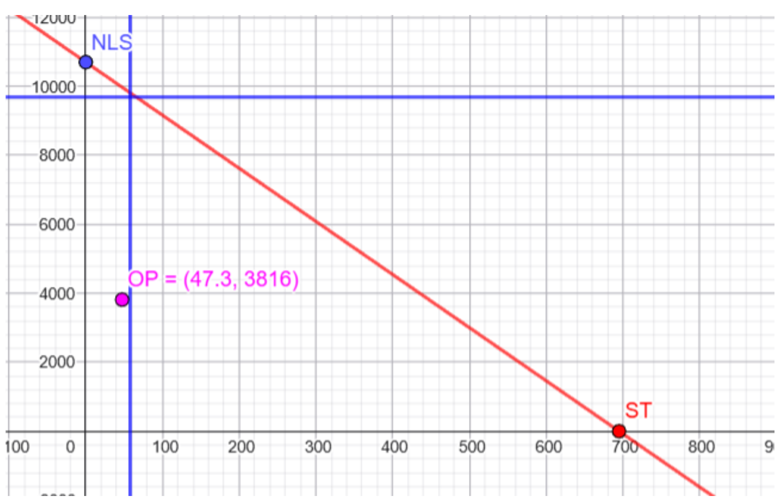

Figure E.6 – Speed-Torque diagram of the motor

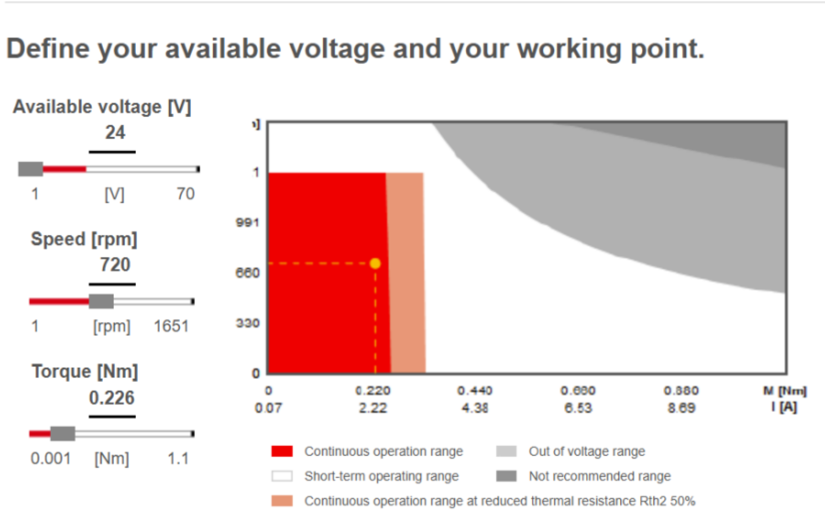

Figure E.7 - Speed-Torque plot of the Motor & Gearbox (Maxon Configurator)